Geochemistry Geophysics Geosystems G3
AN ELECTRONIC JOURNAL OF THE EARTH SCIENCES
Published by AGU and the Geochemical Society

Article
Volume 8, Number 6
28 June 2007
Q06014, doi:10.1029/2006GC001449
ISSN: 1525-2027

Constraints on Hadean zircon protoliths from oxygen isotopes, Ti-thermometry, and rare earth elements

Dustin Trail
Department of Geological Sciences and Center for Astrobiology, University of Colorado, Boulder, Colorado 80309-0399, USA

Now at Department of Earth and Environmental Sciences, Rensselaer Polytechnic Institute, Troy, New York 12180, USA (traild@rpi.edu)

Stephen J. Mojzsis
Department of Geological Sciences and Center for Astrobiology, University of Colorado, Boulder, Colorado 80309-0399, USA

T. Mark Harrison
Research School of Earth Sciences, Australian National University, Canberra, ACT 0200, Australia

Department of Earth and Space Sciences and Institute of Geophysics and Planetary Physics, University of California, Los Angeles, California 90095, USA

Axel K. Schmitt
Department of Earth and Space Sciences and Institute of Geophysics and Planetary Physics, University of California, Los Angeles, California 90095, USA

E. Bruce Watson
Department of Earth and Environmental Sciences, Rensselaer Polytechnic Institute, Troy, New York 12180, USA

Edward D. Young
Department of Earth and Space Sciences and Institute of Geophysics and Planetary Physics, University of California, Los Angeles, California 90095, USA

[1] We report zircon oxygen isotope ratios and reconnaissance Ti-in-zircon concentrations, guided by cathodoluminescence image studies, for detrital zircons up to 4.34 Ga from the Narryer Gneiss Complex of Western Australia. Zircon oxygen isotope results bolster the view that some Hadean (>3.85 Ga) zircon source melts were enriched in heavy oxygen, a sensitive proxy for melt contamination by sediments altered in liquid water. Zircon crystallization temperatures calculated from Ti concentration in pre-3.8 Ga zircons yield values around 680°C in all cases except for one lower value in a 4.0 Ga grain. Elevated zircon $\delta^{18}O$ values reported here and elsewhere, combined with low minimum-melt crystallization temperatures, and analysis of zircon/melt partitioning of rare earth elements (REEs) provide mutually consistent lines of evidence that the Hadean Earth supported an evolved rock cycle which included formation of granitic water-saturated melts, extensive continental crust, hydrosphere-lithosphere interactions, and sediment recycling within the first 150 million years of planet formation.

Components: 14,639 words, 6 figures, 3 tables.

Keywords: Hadean; crust; ion microprobe; oxygen; zircon thermometry; rare earth elements.

Index Terms: 1009 Geochemistry: Geochemical modeling (3610, 8410); 1020 Geochemistry: Composition of the continental crust; 1065 Geochemistry: Major and trace element geochemistry; 1041 Geochemistry: Stable isotope geochemistry (0454, 4870); 1042 Geochemistry: Mineral and crystal chemistry (3620).

Received 17 August 2006; **Revised** 16 February 2007; **Accepted** 15 March 2007; **Published** 28 June 2007.

Trail, D., S. J. Mojzsis, T. M. Harrison, A. K. Schmitt, E. B. Watson, and E. D. Young (2007), Constraints on Hadean zircon protoliths from oxygen isotopes, Ti-thermometry, and rare earth elements, *Geochem. Geophys. Geosyst.*, *8*, Q06014, doi:10.1029/2006GC001449.

1. Introduction

[2] In the apparent absence of a continuous Hadean (pre-3.85 Ga [*Bleeker*, 2004]) geologic record on Earth, information bearing on the formation and evolution of the earliest crust has traditionally relied on geodynamical model studies [*Reymer and Schubert*, 1985], and broad comparisons with lunar data [*Tera et al.*, 1974]. Additional inferences have been made from pervasively altered [*Moorbath et al.*, 1997; *Sano et al.*, 1999] circa 4.0 Ga granitoid-gneiss terranes [*Bowring and Williams*, 1999; *Iizuka et al.*, 2006] and geochemical analyses of pre-4.0 Ga detrital zircons from Western Australia [e.g., *Maas et al.*, 1992; *Mojzsis et al.*, 2001; *Watson and Harrison*, 2005]. Abundant occurrences of detrital Hadean zircons that comprise up to several percent of the total zircon population in some quartzitic metasediments have been documented from the Mount Narryer (MN) [*Froude et al.*, 1983] and Jack Hills (JH) [*Compston and Pidgeon*, 1986] localities of the Narryer Gneiss Complex (NGC), at the northwestern edge of the Yilgarn Craton in Western Australia [e.g., *Pidgeon and Wilde*, 1998]. The Hadean zircons provide an excellent resource to explore the earliest Earth since zircon is refractory and resistant to chemical alteration and physical breakdown during weathering. Non-metamict crystals can serve as robust repositories of Pb* [*Cherniak and Watson*, 2000], oxygen isotopes [*Valley*, 2003], Hf isotopes [*Cherniak et al.*, 1997] and radiogenic Xe [*Turner et al.*, 2004] (compare to Nd isotopes [*Caro et al.*, 2006]) even in crystals that predate the start of the known terrestrial rock record [e.g., *Harrison et al.*, 2005a].

[3] If zircon retains primary oxygen isotopes from the time of crystallization, such values can be used to place broad constraints on Hadean zircon magmatic sources [e.g., *Mojzsis et al.*, 2001; *Cavosie et al.*, 2005]. This is because empirically-derived zircon/melt oxygen isotopic fractionation factors [*Valley et al.*, 2003] can constrain bulk protolith magma sources and magmatic evolution [*Taylor*, 1968; *Taylor and Sheppard*, 1986]. Zircon oxygen isotope compositions occupy a large range of $^{18}O/^{16}O$ ratios [*Valley et al.*, 2005]. It is generally accepted that deviation of crustal zircon from mantle $\delta^{18}O_{VSMOW}$ values (+5.3 ± 0.3‰ [*Valley*, 2003]) indicates its source melts were in chemical communication with a reservoir enriched (or depleted) in ^{18}O, and the only natural system that can impart such signatures is liquid water interacting with crust at or near Earth's surface. As reviewed by *Valley et al.* [2005], magmatic zircon $\delta^{18}O$ values derived from remelted hydrothermally altered rhyolites from Yellowstone are as low as −0.4‰, and measurements as high as +13.5‰ have been reported from a quartz monzonite from the Frontenac Arch Crow Lake Pluton in Ontario. Non-magmatic $\delta^{18}O$ zircon values as low as −11‰ are documented for hydrothermally altered rocks from the Dabie-Sulu orogen in China that later underwent ultra-high-pressure metamorphism [*Zheng et al.*, 2003]. Oxygen isotope values up to +15‰ for circa 3650 Ma metamorphic zircons in granulite facies supracrustal enclaves (quartz-garnet biotite schists) from the Færinghavn terrane of southern West Greenland [*Cates and Mojzsis*, 2006], and from a discordant overgrowth of a Hadean Jack Hills zircon [*Mojzsis et al.*, 2001] have also been reported.

[4] Oxygen-18 enrichments relative to mantle values measured for core regions in pre-3.8 Ga zircons have been interpreted by a number of workers to indicate an evolved rock cycle and derivation from "S-type" granitoid melts in the Hadean [*Mojzsis et al.*, 2001; *Peck et al.*, 2001;

Valley et al., 2002; *Cavosie et al.*, 2005]. However, alternative views have been proposed that provide different explanations for the Hadean zircon data. For example, oxygen isotope analyses of eight pre-4.2 Ga zircons by *Nemchin et al.* [2006a] yielded values broadly within the terrestrial mantle field and led them to conclude that there was insufficient evidence for a "cool early Earth" between ~4.4–4.0 Ga as advocated by *Valley et al.* [2002]. Instead, *Nemchin et al.* [2006a] drew generic parallels with their Jack Hills zircon analyses and results from a separate study of lunar zircons [*Nemchin et al.*, 2006b] to presume that oxygen isotopes in zircons provide no unique evidence for crust-hydrosphere interactions prior to ~4.0 Ga.

[5] Titanium concentration in zircon ($[Ti]_{zircon}$) is a geochemical tracer with potential to constrain zircon crystallization temperature. Recent $[Ti]_{zircon}$ results for 4.35–4.0 Ga Jack Hills zircons indicate formation temperatures that cluster around 680°C [*Watson and Harrison*, 2005, 2006]. The $[Ti]_{zircon}$ thermometer presupposes coexistence of rutile (essentially pure TiO_2) with zircon at crystallization. On the basis of measured $[Ti]_{zircon}$, an equilibrium constant can be calculated from the activity of TiO_2 in zircon by assuming an activity of rutile equal to ~1 [*Watson and Harrison*, 2005]. The $[Ti]_{zircon}$ thermometer has been calibrated experimentally for high (1025–1450°C) temperatures, and natural zircons have been used for crystallization temperatures of ~580°C–1170°C [*Watson et al.*, 2006]. The retention of tetravalent Ti in zircon is aided by the fact that it substitutes without charge compensation most favorably into the Si^{4+} site [*Harrison et al.*, 2005b; *Ferry and Watson*, 2007].

[6] *Maas et al.* [1992] reported rare earth element (REE) patterns in individual JH and MN zircons which show that some grains are markedly enriched in LREE contents and are similar to zircons from Phanerozoic diorites and granites. Follow-up studies presented $\delta^{18}O$ data in concert with REE data, showing high $\delta^{18}O$ values as well as enriched LREEs, which substantiate earlier conclusions that the chemistry of JH grains are consistent with zircons derived from granitoid-type source rocks [*Peck et al.*, 2001; compare to *Coogan and Hinton*, 2006]. In another study, trace element patterns and U concentrations of detrital zircons from Mount Narryer were used to argue that these particular grains were derived from evolved granitic rocks [*Crowley et al.*, 2005].

[7] Geochemical tracers in zircon such as oxygen isotope ratios, Ti thermometry, and analysis of zircon/melt partitioning of REEs can be used to constrain zircon paragenesis in the absence of their parent rocks. For example, were Hadean zircon protoliths dominantly of low temperature granite-type or instead the product of relatively high-temperature mafic/ultramafic melts? Here, we present new oxygen isotope data for 89 pre-3.8 Ga grains previously characterized by U-Pb ion microprobe geochronology [*Harrison et al.*, 2005a]. In addition, multiple Ti_{zircon} measurements were made for a subset (n = 13) of the pre-3.8 Ga grains. Our new Ti concentrations for zircons correspond to temperatures around 680°C, consistent with granite formation under conditions akin to wet minimum-melts [*Watson and Harrison*, 2005]. Moreover, our REE modeling demonstrates that Hadean zircons are dominantly of felsic magmatic provenance. These observations complement recent Hf isotope data from individual Hadean zircons that appear to be consistent with the establishment of significant continental crust and active plate boundary processes within the first 150 million years of Earth formation [*Harrison et al.*, 2005a, 2006].

2. Samples and Methods

[8] Samples JH992 [*Mojzsis et al.*, 2001] and ANU [*Harrison et al.*, 2005a] were collected from the original locality (S26° 10.09′, E116° 59.39′) where pre-4.0 Ga Jack Hills zircons were first discovered [*Compston and Pidgeon*, 1986]. Additionally, a new sample was included from a separate rock outcrop (JH0101) ~250 m west along strike from the JH992 locality, which preserved stream bedform and scour features with bands rich in heavy minerals. Mount Narryer sample MN0102 (S26° 30.90′, E116° 22.80′) was a ~3 kg specimen that contained cm-scale clasts of banded iron-formation (BIF) visible in hand sample. Zircons were concentrated using standard heavy liquid techniques. Sieved samples were first treated with hand magnet and isodynamic Frantz magnetic separator (~1.5 A) to remove magnetic fractions prior to heavy liquid separations. After cleaning in acetone and deionized water (DI H_2O), zircons picked from the heavy mineral separates were mounted on double-sided adhesive tape and cast in 2.5 cm epoxy discs. Grain cross sections of individual zircons exposed during polishing were brought to optical finish using 0.05 μm alumina paste.

2.1. Zircon Oxygen Isotope Determination by Ion Microprobe Multicollection

[9] All high spatial resolution $\delta^{18}O$ zircon determinations were made using the UCLA CAMECA ims 1270 high-resolution ion microprobe in Faraday multicollection mode [e.g., *Mojzsis et al.*, 2001; *Booth et al.*, 2005] with regular monitoring of background count rates on the detectors. In all analyses a liquid nitrogen cold finger was used to remove trace condensable gases from the sample chamber. A ~5 nA Cs^+ beam was focused to a ~20 μm spot and 10 keV secondary ions were admitted to the mass spectrometer after passing through a 30 eV energy slit. Mass spectrometer entrance and exit slits were tuned to a mass resolving power of ~2400 to resolve hydride interferences such as $H_2^{16}O^-$. Under these conditions, average count rates for $^{16}O^-$ and $^{18}O^-$ were ~2×10^9 and ~4×10^6 cps, respectively. Zircons were presputtered for 1 min, and the total integration time per analysis was 5 min. Errors based on counting statistics are 0.1‰ or less in almost all cases (compare to ANU32_1-7@2). The $^{16}O^-$ and $^{18}O^-$ signals were corrected for shifts in the baseline of the Faraday cup detector system from intermittent measurements with the primary and electron beams blanked.

[10] Obvious cracks and metamict regions of individual zircon grains were avoided during analysis, but postanalysis inspection by reflected light (RL), backscatter electron (BSE) or cathodoluminescence imaging (CL) was used to scrutinize (and in some cases exclude from further consideration) problematic analysis spots [e.g., *Cavosie et al.*, 2005]. Cracks and defect structures in zircons are well-known conduits for contaminants [e.g., *Peck et al.*, 2001]. They may act as gateways for diffusive exchange and it is not inconceivable that mount media may seep into microcracks. To explore for oxygen isotope trends in variably altered samples, zircons with variable degrees of Pb-loss (quantified by U-Pb discordance) were analyzed. Exact protocols varied from mount-to-mount (n = 12) and these can be classified into three groups.

[11] 1. Sample mount ANU29 was analyzed for oxygen isotopes without prior removal of existing geochronology spots by repolishing. This was done so that analysis spots for in situ oxygen isotopes could be placed adjacent to geochronology spots without overlap. One possible objection to this approach is that the oxygen beam from the duoplasmatron source embeds ^{16}O into zircon regions that may result in anomalously low $\delta^{18}O$ values [*Benninghoven et al.*, 1987]. We note, however, that this is an extremely local effect (<30 μm) and it was considered of sufficient benefit to analyze a sample mount in this manner.

[12] 2. Zircons in sample mount JH992CU11 were rapidly characterized for $^{207}Pb/^{206}Pb$ ages in "survey mode" following our usual techniques [*Mojzsis et al.*, 2001; *Turner et al.*, 2004; *Harrison et al.*, 2005a]. This procedure was used to identify potentially ancient grains (>3.8 Ga) in a fraction of the time required for a full 10 cycle U-Pb geochronology analysis (~10 min). Subsequently, JH992CU11 was repolished to completely remove all prior ion microprobe pits, cleaned in 1N HCl and DI water baths, Au-coated and measured for oxygen isotopes. After oxygen isotope determinations, U-Pb ion microprobe geochronology analyses were performed precisely in the same place as oxygen isotope measurements.

[13] 3. For all other samples analyzed in this study, zircons were characterized in survey mode, followed by U-Pb geochronology as in (1), except a hand polish followed age determination to remove any trace of preexisting ion microprobe geochronology spots before measurement for oxygen isotopes.

[14] Instrumental mass fractionation (Δ_{imf}), the difference between the actual $^{18}O/^{16}O$ of standard grains and that measured by secondary ion mass spectrometry, varied from 1 to 2 per mil (‰). Some of these Δ_{imf} variations are probably associated with slight changes in the geometry of the sample mount after exchange from the sample chamber. To monitor this effect, we collected standard data for each sample mount. Because Δ_{imf} is sensitive to secondary ion generation and extraction conditions related to the geometry of individual mounts, it is crucial to have standard materials cast with the unknowns on the same sample mount. Duluth gabbro zircon AS-3 [*Paces and Miller*, 1993] is a widely used and abundant geochronology standard [e.g., *Schmitz et al.*, 2003] and has also been used for SIMS oxygen isotope calibration [*Booth et al.*, 2005]. The AS-3 zircon is routinely included on all of our sample mounts. Our standardization protocol calls for an average of 10 individual standard measurements per mount, leading to an average external precision of ±0.7‰, and in most cases measurements were performed on more than one AS-3 grain per mount (auxiliary material[1] Tables S1 and S2). Overall, standards measurements comprised >60% of all analyses performed.

[1] Auxiliary material data sets are available at ftp://ftp.agu.org/apend/gc/2006gc001449. Other auxiliary material files are in the HTML.

[15] To evaluate whether Δ_{imf} tracks with compositional variations as "matrix effects" in zircon, we intermittently measured standards KIM-5 ($\delta^{18}O$ = +5.09‰ [*Valley*, 2003]) and 91500 ($\delta^{18}O$ = +9.86‰ [*Wiedenbeck et al.*, 2004]) with AS-3 (+5.34‰; see section 2.2) cast together on a separate standard mount. Matrix effects in oxygen isotopes were not observed within the analytic precision of the ion microprobe for three different standard zircons with HfO_2 values of 0.695 wt.% (91500 [*Wiedenbeck et al.*, 2004]), 1.20 wt.% (AS-3 [*Black et al.*, 2004]), and 1.23 wt.% (KIM-5 [*Valley et al.*, 2003]). The HfO_2 abundance in our primary zircon standard (AS-3) is similar to JH and MN zircon compositions [*Cavosie et al.*, 2005; *Maas et al.*, 1992; *Crowley et al.*, 2005]. *Nemchin et al.* [2006b] applied Hf-related matrix effects corrections which were originally derived for high-energy-offset analyses [*Peck et al.*, 2001], in contrast to their low-energy-offsets. In the absence of observable matrix effects on our zircon standards, we applied no additional matrix effects corrections to the data.

[16] In reflected and transmitted light microscopy, it was apparent that some AS-3 standard grains mounted with the unknowns host inclusions and crack ingrowths of secondary phases such as Fe-oxide. However, secondary features are readily identifiable in optical images used to create maps of the sample mounts, and are easily avoided during analysis. Hence we found no reason to reject any standard analyses.

[17] Internal and external analysis errors are reported for unknowns, the latter propagating the variability of the AS-3 standard measurements for each mount. Detector background subtraction for ^{18}O was made by interpolation of bracketed background measurements with the time-stamp of each analysis for standards and unknowns. Corrections for background on ^{16}O were deemed unnecessary due to high count rates ($\sim 10^9$ cps) for zircon analyses relative to background fluctuations ($\sim 10^3$ cps). For each analytical session (reported in Table S1), we calculated the weighted mean of the background corrected standard $^{18}O/^{16}O$ ratios (Table S2). The final zircon $\delta^{18}O_{VSMOW}$ was calculated according to the relation:

$$\sigma^{18}O_{VSMOW}(zircon) = \left[\frac{\left(^{18}O/^{16}O\right)_{unkwn}}{\left(^{18}O/^{16}O\right)_{STD\_meas}/(^{18}O/^{16}O)_{STD\_true}} - VSMOW \right] \bullet \frac{1000}{VSMOW} \quad (1)$$

Table 1. Laser Fluorination Analyses of Oxygen Isotope Ratios of AS-3 Zircon

	wt, mg	$\delta^{17}O$	$\delta^{18}O$	$\Delta^{17}O$
Aliquot 1	0.58	2.801	5.368	0.010
Aliquot 2	0.65	2.762	5.319	−0.004
		$\delta^{18}O_{ave}$ =	5.344 ± 0.035	

where $^{18}O/^{16}O_{unkwn}$ is the measured unknown background corrected ratio, $^{18}O/^{16}O_{STD\_meas}$ is the average measured standard value on a given mount (Table S1), $^{18}O/^{16}O_{STD\_true}$ is the true value of the standard (AS-3 = 0.0020159) and VSMOW = 0.0020052.

[18] As a follow-up to the unusually high $\delta^{18}O$ zircon values previously reported for grain JH992_42 (core = +10‰, rim = +15‰) by *Mojzsis et al.* [2001], and as a means to simultaneously test for volume homogeneity in oxygen isotopes and agreement between our results and that of earlier studies, this zircon was removed from its original mount with an unpolished prism face placed face down in adhesive tape and recast with AS-3, KIM-5, and 91500. Results of this analysis are presented in section 3.

2.2. Laser-Fluorination Oxygen Isotope Analyses of Standard Zircon AS-3

[19] To prepare zircon standard AS-3 for oxygen isotopic analysis via laser fluorination, we hand-picked ~200 inclusion-free grains, separated by standard heavy-mineral techniques from a fresh sample of the original Duluth gabbro. This was done with the view that optically "pure" whole grains are probably reasonable approximations to visibly homogenous regions of the polished AS-3 surfaces chosen for analysis by ion microprobe. Splits of AS-3 were separated into 0.58 and 0.65 mg aliquots and fluorinated by infrared laser heating. Oxygen isotope ratios were analyzed with a Finnigan Delta Plus gas ratio mass spectrometer (UCLA) and absolute $\delta^{18}O$ zircon values were calibrated against the San Carlos olivine silicate standard (+5.3‰) and globally homogeneous tropospheric O_2 [e.g., *Young et al.*, 1998]. Results in Table 1 use the average $\delta^{18}O$ value of +5.34 ± 0.03‰ (1σ) for standard AS-3. Our data are in excellent agreement with separate $\delta^{18}O$ zircon laser fluorination results on Duluth gabbro zircons (+5.21 ± 0.34‰) reported by *Booth et al.* [2005].

Table 2. Ion Microprobe Analyses of Oxygen Isotope Ratios of Jack Hills and Mt. Narryer Zircons

Grain and Spot	$^{207}Pb/^{206}Pb$ Age, Ma	% Concord	Measured $^{18}O/^{16}O$		1σ (Internal)	Background Corrected $^{18}O/^{16}O$	$\delta^{18}O_{CALC}$		1σ (External)	Correlative to Age?
ANU29[a]										
1-15@1	4036	94	0.0020251	±	1.40E-07	0.0020235	6.7	±	0.9	y
1-15@2			0.0020245	±	1.50E-07	0.0020228	6.4	±	0.9	n
11-7@1	3979	95	0.0020262	±	2.00E-07	0.0020247	7.3	±	0.9	n
11-9@2	3860	97	0.0020235	±	1.60E-07	0.0020219	5.9	±	0.9	n
11-10@1	4012	96	0.0020269	±	1.70E-07	0.0020254	7.7	±	0.9	n
12-4@1	4020	98	0.0020253	±	1.50E-07	0.0020238	6.9	±	0.9	y
13-11@1	4142	105	0.0020229	±	2.40E-07	0.0020214	5.7	±	0.9	y
ANU30										
9-1@1	4340	94	0.0020193	±	3.40E-07	0.0020181	5.1	±	0.8	y
9-1@2			0.0020200	±	1.40E-07	0.0020186	6.9	±	0.7	n
ANU31										
1-14@1	4034	96	0.0020207	±	2.54E-07	0.0020200	5.1	±	0.9	y
3-11@1			0.0020174	±	1.50E-07	0.0020156	5.2	±	0.2	n
3-11@2	3947	95	0.0020192	±	1.60E-07	0.0020173	6.1	±	0.2	y
4-10@1	4118	93	0.0020206	±	1.70E-07	0.0020198	5.0	±	0.9	y
4-14@1	4121	93	0.0020194	±	1.00E-07	0.0020185	4.4	±	0.9	y
5-1@1	4058	94	0.0020193	±	2.80E-07	0.0020186	4.4	±	0.9	y
7-5@1	3981	95	0.0020207	±	1.70E-07	0.0020200	5.1	±	0.9	y
8-4@1	4111	94	0.0020198	±	1.90E-07	0.0020190	4.6	±	0.9	y
10-11@1	4040	93	0.0020196	±	2.10E-07	0.0020189	4.6	±	0.9	y
12-12@1	4064	93	0.0020214	±	2.10E-07	0.0020207	5.5	±	0.9	y
14-3@1	4121	95	0.0020223	±	2.00E-07	0.0020216	5.9	±	0.9	y
14-7@1	4127	93	0.0020229	±	2.20E-07	0.0020221	6.2	±	0.9	y
15-8@1	4111	95	0.0020216	±	1.30E-07	0.0020208	5.5	±	0.9	y
ANU32										
1-7@1	4021	92	0.0020182	±	2.10E-07	0.0020170	5.5	±	0.6	y
1-7@2			0.0020283	±	1.60E-06	0.0020269	10.5	±	0.8[b]	n
2-15@1	4012	93	0.0020190	±	1.80E-07	0.0020179	5.9	±	0.6	y
2-15@2			0.0020199	±	1.30E-07	0.0020188	6.4	±	0.6	n
6-9@1	4070	95	0.0020185	±	1.40E-07	0.0020174	5.7	±	0.6	y
6-10@1			0.0020189	±	1.40E-07	0.0020178	5.9	±	0.6	y
6-10@2	4152	91	0.0020194	±	1.50E-07	0.0020183	6.1	±	0.6	y
6-15@1	4092	92	0.0020189	±	1.20E-07	0.0020178	5.9	±	0.6	y
6-15@2			0.0020208	±	1.80E-07	0.0020197	6.8	±	0.6	y
8-13@1	3993	94	0.0020184	±	1.60E-07	0.0020174	5.7	±	0.6	y
11-5@1	4068	94	0.0020130	±	1.80E-07	0.0020118	2.9	±	0.6	y
11-5@2			0.0020196	±	1.40E-07	0.0020186	6.3	±	0.6	y
ANU33										
1-4@1	3995	92	0.0020200	±	1.50E-07	0.0020186	5.6	±	0.8	y
5-2@1	3929	97	0.0020194	±	1.40E-07	0.0020181	5.3	±	0.8	y
5-3@1	4054	95	0.0020194	±	1.30E-07	0.0020181	5.3	±	0.8	y
6-14@1	4065	91	0.0020227	±	1.80E-07	0.0020212	6.8	±	0.8	n
7-3@1	3994	96	0.0020200	±	1.50E-07	0.0020186	5.6	±	0.8	y
7-15@1	4004	98	0.0020215	±	1.60E-07	0.0020200	6.2	±	0.8	y
8-1@1	3995	93	0.0020191	±	1.70E-07	0.0020178	5.1	±	0.8	y
8-1@2			0.0020207	±	1.50E-07	0.0020194	6.0	±	0.8	n
11-15@1			0.0020230	±	1.50E-07	0.0020215	7.0	±	0.8	n
11-15@2	4117	96	0.0020210	±	1.80E-07	0.0020196	6.0	±	0.8	y
12-7@1	3903	97	0.0020218	±	1.50E-07	0.0020204	6.5	±	0.8	y
12-14@1	4001	97	0.0020221	±	1.30E-07	0.0020206	6.6	±	0.8	y
12-14@2			0.0020240	±	1.30E-07	0.0020226	7.5	±	0.8	n
13-6@1	4063	92	0.0020205	±	1.40E-07	0.0020191	5.8	±	0.8	y
14-9@1	4084	95	0.0020213	±	1.40E-07	0.0020199	6.2	±	0.8	y
15-11@1	4196	96	0.0020218	±	1.50E-07	0.0020204	6.4	±	0.8	y
15-11@2			0.0020231	±	1.40E-07	0.0020217	7.1	±	0.8	n
JH0101-1										
6-10@1	3919	94	0.0020179	±	1.60E-07	0.0020170	5.8	±	1.0	y
9-18@2	3811	98	0.0020181	±	1.30E-07	0.0020153	5.0	±	1.0	y
9-20@1	3925	92	0.0020141	±	1.20E-07	0.0020131	3.9	±	1.0	y

Table 2. (continued)

Grain and Spot	$^{207}Pb/^{206}Pb$ Age, Ma	% Concord	Measured $^{18}O/^{16}O$		1σ (Internal)	Background Corrected $^{18}O/^{16}O$	$\delta^{18}O_{CALC}$		1σ (External)	Correlative to Age?
9-20@3			0.0020137	±	1.10E-07	0.0020126	3.6	±	1.0	n
10-4@1	3852	95	0.0020183	±	1.90E-07	0.0020172	5.9	±	1.0	y
JH0101-CC01										
2-3@3	4091	100	0.0020175	±	1.60E-07	0.0020162	5.0	±	0.7	y
2-3@4			0.0020186	±	9.70E-08	0.0020174	5.6	±	0.7	y
JH0101-2										
3-15@1	4230	99	0.0020207	±	1.10E-07	0.0020191	5.7	±	1.0	y
7-18@1	4091	99	0.0020193	±	1.40E-07	0.0020176	4.9	±	1.0	y
10-17@1	4074	100	0.0020188	±	1.10E-07	0.0020174	4.8	±	1.0	y
10-17@2			0.0020171	±	1.30E-07	0.0020157	3.9	±	1.0	n
MN0102-1 (grains located in matrix) collected from Mount Narryer										
1-1@1	4042	99	0.0020132	±	1.20E-07	0.0020119	5.5	±	0.2	y
2-7@1	4137	103	0.0020125	±	1.50E-07	0.0020112	5.1	±	0.2	y
2-7@2	4113	97	0.0020133	±	1.30E-07	0.0020119	5.5	±	0.2	y
JH992CU11[c]										
2-10@2	3863	107	0.0020225	±	1.29E-07	0.0020221	6.8	±	0.4	y
4-8@1	4083	99	0.0020211	±	1.30E-07	0.0020206	6.1	±	0.4	y
4-8@2	4076	105	0.0020203	±	1.60E-07	0.0020198	5.7	±	0.4	y
4-9@2	4017	101	0.0020205	±	9.10E-08	0.0020200	5.8	±	0.4	y
6-10@1	4110	99	0.0020201	±	1.10E-07	0.0020195	5.5	±	0.4	y
8-6@1	4126	94	0.0020208	±	1.90E-07	0.0020202	5.8	±	0.4	y
8-6@2	4133	94	0.0020200	±	9.80E-08	0.0020194	5.5	±	0.4	y

[a] Sample unpolished prior to oxygen isotope analyses.
[b] Internal error is greater than external error.
[c] Oxygen work performed prior to geochronology.

2.3. Ti-in-Zircon Concentrations

[20] Titanium concentrations in zircon were measured using the same protocol as *Watson et al.* [2006]; a brief summary is provided. Data for $[Ti]_{zircon}$ were collected with a CAMECA ims 3f ion microprobe at Woods Hole Oceanographic Institution. Duplicate measurements on pre-4.0 Ga zircons for two mounts (JH0101-2 and JH992-CU11) were made at different grain locations. A primary 5 nA O^- beam was focused to a 15–20 μm spot on synthetic zircon standards of known Ti concentrations as determined by electron microprobe. Synthetic zircons grown at high temperatures (~1400°C) and characterized for their Ti concentrations by electron microprobe were used with natural samples as ion microprobe standards. The combined electron and ion microprobe analytical uncertainty for zircons crystallizing in the 650–700°C range relevant to this study is ~5°C (1σ). Minimum detection limits for Ti by this method are ~0.1 ppm. The measured concentrations applied to the equation define a log linear dependence of Ti with temperature as presented by *Watson et al.* [2006]. The uncertainties on the constants of the thermometry equation propagate an error of ~5°C (1σ) for temperatures reported here. When it was possible to do so, cracks were avoided because it has been found that measured Ti concentrations are often elevated when analyses occur on cracks in zircon [*Watson and Harrison*, 2005; *Watson et al.*, 2006].

3. Results

3.1. Hadean Zircon Oxygen Isotopes and CL Imagery

[21] We analyzed 89 JH and MN zircons with a total of 139 separate oxygen spots; many measurements can be directly correlated with the locations of previously documented U-Pb geochronological analyses. The 72 spot data identified as analytically reliable on the basis of the absence of cracks and inclusions at the measurement location are reported in Table 2. These data comprise measured pre-background-corrected and post-background-corrected $^{18}O/^{16}O$ ratios, zircon $\delta^{18}O$ for the unknowns and results for ≤10% discordant geochronology spots collected in the vicinity of the oxygen spots. All O-isotope measurements made during our four day ion microprobe session (with standards and

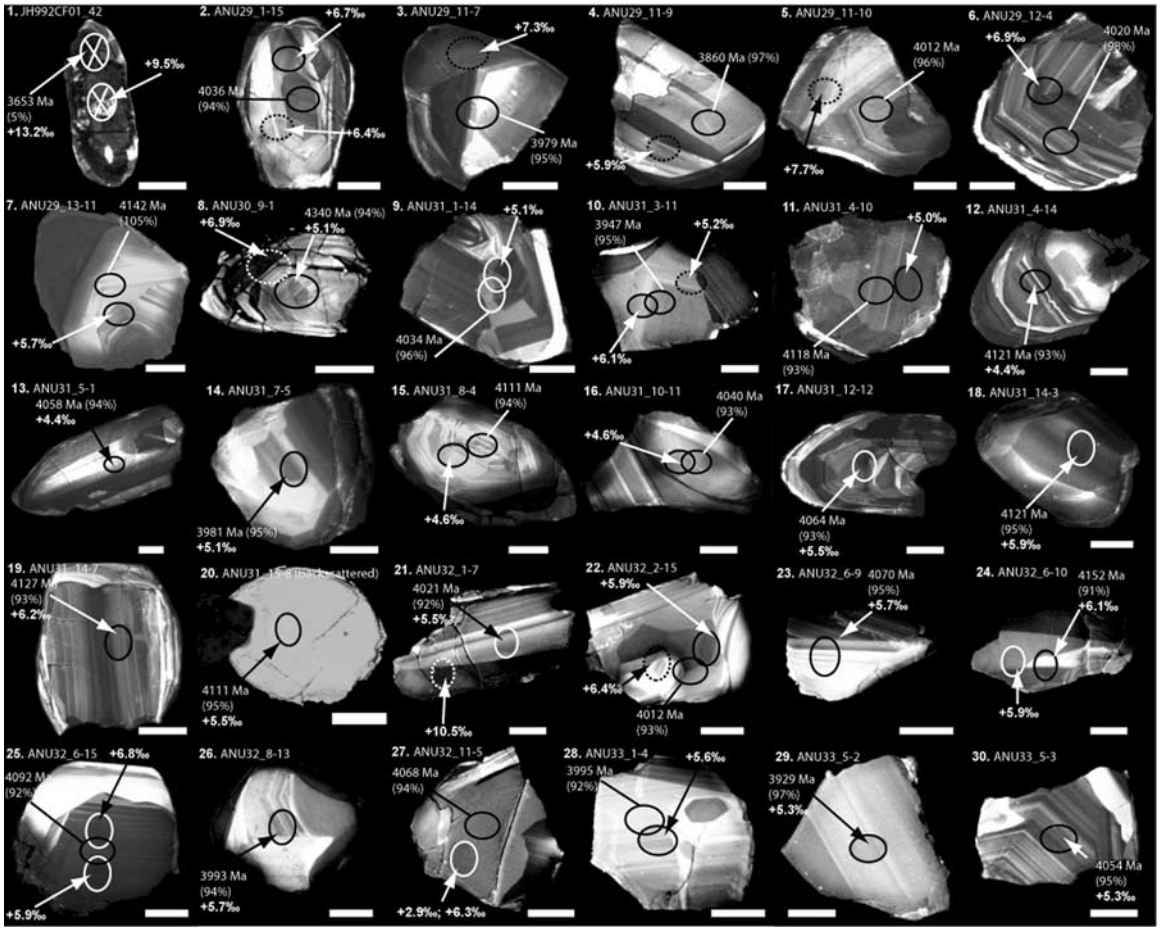

Figure 1. Cathodoluminescence images of zircons in Table 2 with geochronology and oxygen data. Ion microprobe spots with an "X" represent an analysis on a crack or on a discordant grain region, and dashed ion microprobe spots represent an analysis free of analytical artifacts, but which cannot be correlated with age. All zircons contain at least 1 geochronology spot >90% concordant except for JH992_42, which is shown as a follow-up and a confirmation of previous work [*Mojzsis et al.*, 2001]. Grain ANU31_15-8 was inadvertently not imaged in CL. Boxed images contain Ti temperature measurements (section 3.3).

data subsequently rejected on the basis of the criteria outlined above) are reported in auxiliary material Table S2. Sample data for analyses on grain cracks, <90% concordant zircons, and/or grains younger than 3800 Ma are tabulated separately in auxiliary material Table S3. Cathodoluminescence images for Hadean grains which were analyzed on grain cracks can be found in Figure S1. Data free of analytical artifacts (Table 2) display a peak in $\delta^{18}O$ at +5.8‰ that is similar to the average of 28 analysis spots on eight pre-4.2 Ga zircons reported by *Nemchin et al.* [2006a], and lower by ~0.4‰ when compared to the 41 zircons standardized with KIM-5 from *Cavosie et al.* [2005]. The reason for the difference between our results and *Cavosie et al.* [2005] may be due to $\delta^{18}O$ zircon heterogeneity among samples, but analytical bias due to different procedures in the oxygen standardization (or the standard itself) cannot be excluded.

[22] In order to assess whether these differences in oxygen isotope values are statistically significant, we have used the Kolmogorov-Smirnov (K-S) test to compare zircon $\delta^{18}O$ values of individual studies. The K-S test has been widely used in Earth Sciences [e.g., *Miller and Kahn*, 1962], and is advantageous because unlike the "t-test" it is distribution free. In our analysis, we used the Gaussian kernel probability function described by *Silverman* [1986]. In addition, our comparison takes into consideration the external error for each zircon. Results indicate that data from Table 2 and *Nemchin et al.* [2006a] fulfill the requirements of a single population of oxygen isotope values in the

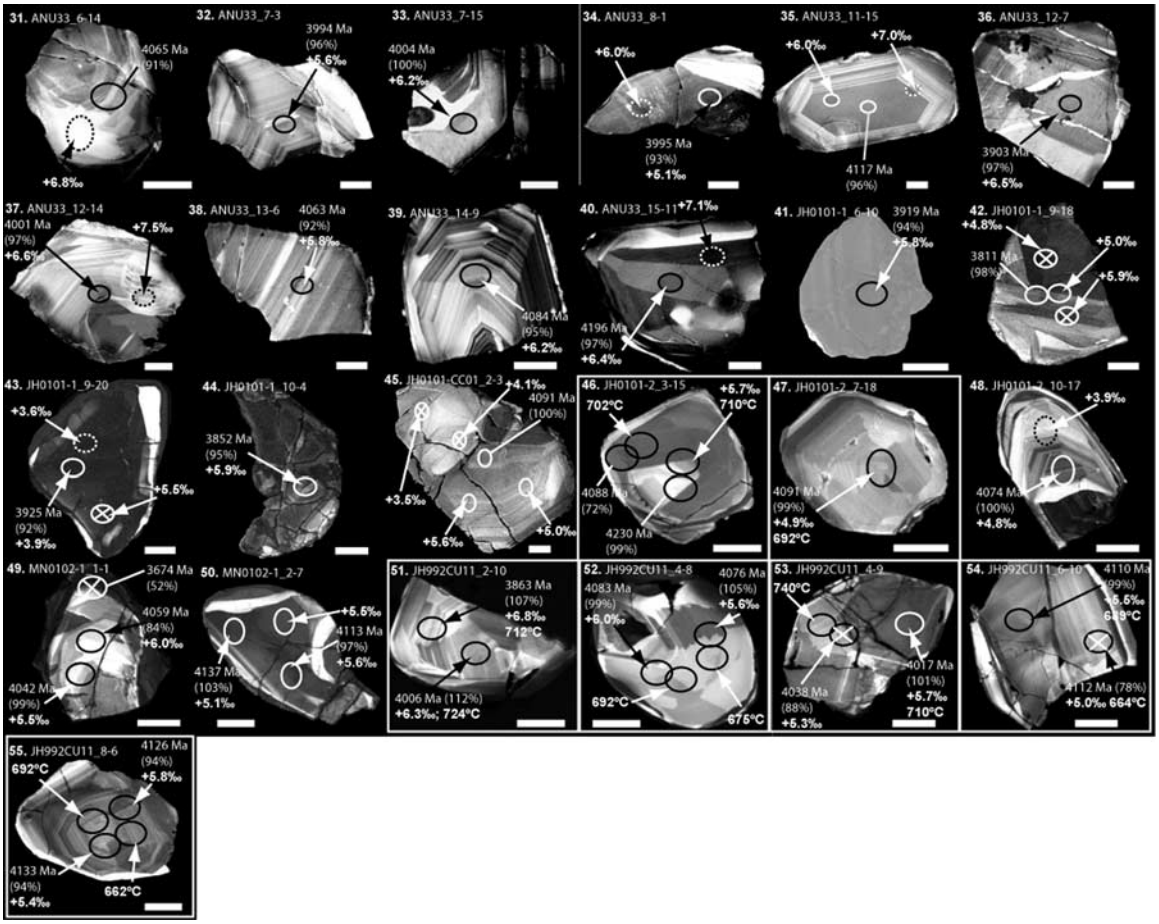

Figure 1. (continued)

Hadean zircons at the 95% confidence level. However, when our data are compared to the data set of *Cavosie et al.* [2005], the probability that the zircons were derived from the same population is <5%. Despite these differences, our results validate previous findings that Hadean zircons on average are enriched above mantle equilibrium values.

[23] For two of our zircon grains, the Cs-ion beam used for oxygen isotope measurements overlapped unpolished geochronology spots (ANU29_11–9: Figure 1, no. 4; ANU29_10–6: Figure S1, no. 64). As expected, the measured $\delta^{18}O$ values are +2.0‰ and +2.3‰, respectively, which reflects ^{16}O contamination from the $^{16}O_2^-$ ion beam [*Benninghoven et al.*, 1987]. The block data of these two analyses show the expected systematic increase in $^{18}O/^{16}O$ with depth as the contaminant ^{16}O decreases. Such increase is not seen in other measured unknowns where beam spot overlap was avoided, which means that the influence of implanted ^{16}O is negligible outside of the exact locality of the previous analysis spot.

[24] Figure 1 shows CL images labeled with geochronology and oxygen results and analysis spot locations. While some zircons show interpretable core-rim relationships in CL (e.g., Figure 1: no. 2, 6–8, 12, 15, 17, 25, 39, 48, 51, 55), such patterns are diffuse in other cases (e.g., Figure 1: no. 16, 18, 21, 22, 27, 29, 30, 38) and a core/rim assignment to individual spots is ambiguous in many crystals. In light of this observation, Table 2 reports whether the oxygen spot locations can be correlated to geochronology spots on the basis of CL patterns. For example, in Figure 1, no. 35, the geochronology spot and the +6.0‰ oxygen measurement were not made on top of one another, but the similarity of CL patterns supports the interpretation that the two are part of the same grain domain. Zircons outlined by white boxes in Figure 1 were further investigated for Ti thermometry (section 3.3). Data from 50 zircons in Table 2 from 57 ion microprobe oxygen spots from this data set can be directly correlated with U-Pb geochronology. Some zircons were analyzed so that both geochronology and O-isotopes

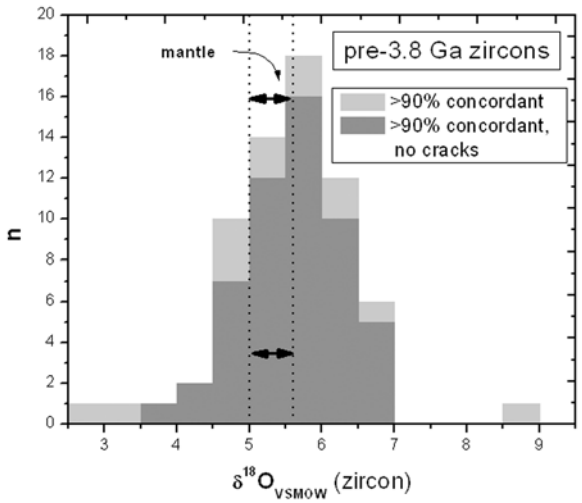

Figure 2. Frequency distribution of $\delta^{18}O_{VSMOW}$ (zircon) measurements of pre-3.8 Ga grains. The distribution is divided into two categories: (1) all zircons measured with a correlative age spot which are at least 90% concordant and (2) all zircons which fall under category 1, but where the $\delta^{18}O$ analysis spot is not located on a grain crack based on detailed retrospective imaging studies. We find that the average oxygen isotopic composition derived for analyses performed on zircons where cracks are present and those without are within 0.1‰ of each other, but the range of $\delta^{18}O$ of grains with cracks is greater.

were collected in the same grain domain after polishing. For analyses where correlated $^{207}Pb/^{206}Pb$ ages can be established, 15 (~25%) yield $\delta^{18}O$ values greater than or equal to 6.0‰ and 5 (~10%) yield values ≥6.5‰.

[25] In Figure 2, two distributions for $\delta^{18}O$ values in zircons ≥3.8 Ga are plotted: (1) ≥90% concordant and (2) ≥90% concordant without cracks on or near oxygen analysis spots. The lowest $\delta^{18}O$ zircon value obtained in our analysis was +2.9‰ (Table 2: ANU32_11-5; Figure 1: no. 27); however, a successive measurement of the same spot recorded a value of +6.3‰. The two highest values we obtained were +10.5‰ (not plotted) measured on a region of grain ANU32_1-7 of uncertain age (Table 2: ANU32_1-7; Figure 1: no. 21) and +8.6‰ on a concordant but cracked grain region (Table S3: JH992CU11_8-6; Figure S1: no. 84).

[26] Our remeasurement of JH992_42 (reported by *Mojzsis et al.* [2001]; Figure 1, no. 1) mounted with AS-3, 91500, and KIM-5 yielded zircon core and rim values that vary slightly with the standard used for instrumental mass fractionation correction: 9.5‰/13.2‰ (AS-3; 1s.e. = ±0.6%), 9.7‰/13.4‰ (91500; 1 s.e. ±1.4‰), and 8.9‰/12.6‰ (KIM-5; 1 s.e. ±0.3‰). The differences in $\delta^{18}O$ zircon instrumental mass fractionation corrections using different standards (all measured on the same mount) are small and agree within error. Because data collected here were taken from an opposite prism face of JH992_42, we find the results in good agreement with the core/rim values of +10‰/+ 15‰ from *Mojzsis et al.* [2001]. However, because this zircon is highly discordant [*Mojzsis et al.*, 2001], we deem it unlikely that this zircon records primary $\delta^{18}O$ values.

3.2. Oxygen Isotope Systematics in Variably Discordant Zircons

[27] To explore for possible zircon oxygen isotope correlations, we analyzed a suite of variably dis-

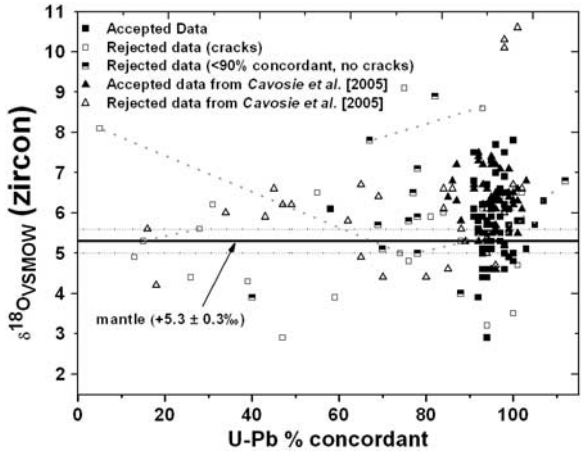

Figure 3. Comparison of zircon $\delta^{18}O_{VSMOW}$ versus U/Pb concordance (%) where correlative $\delta^{18}O$ and geochronology measurements are documented. In this study, zircons with multiple $\delta^{18}O$ versus age spots are connected by (dashed) tie lines. This plot also includes some grains younger than 3800 Ma and reported in Table S3 which are not present in Figure 2. Results have been divided into three categories: (1) analyses on a grain crack (open symbol), (2) analyses on zones greater than 10% discordant (semi-open symbol), and (3) analyses do not meet categories 1 and 2, and are most likely to represent the $\delta^{18}O$ of primary crystallization (closed symbol). Also included in this figure are data from *Cavosie et al.* [2005]. We find that zircons which are more discordant appear to have lower (measured) $\delta^{18}O$ values. The two exceptions are JH992CU11_10-8 and JH992_42, which record values of +8.1‰ and +13.2‰ (off scale), respectively, and both are 5% concordant. This result may be symptomatic of oxygen exchange with the homogenous Jack Hills sediments, where $\delta^{18}O$ values +≥10‰ have been reported [*Cavosie et al.*, 2005].

Table 3. Ion Microprobe Analyses of Ti Concentrations of Jack Hills Zircons

Grain and Spot	$^{49}Ti/^{30}Si$	ppm Ti	T, °C
JH0101-2			
3–15a	0.000115	7	710
3–15b	0.000104	6.3	702
5–11a	0.000022	1.3	588
5–11b	0.000039	2.4	629
5–11c	0.000038	2.3	626
7–18	0.000092	5.6	692
8–8	0.000049	3	645
8–10	0.00011	6.7	707
9–15a	0.000041	2.5	632
9–15b	0.000353	21.4	812[a]
9–15c	0.000139	8.4	726
JH992-CU11			
1–7a	0.000105	6.4	703
1–7b	0.000084	5.1	685
2–10a	0.000118	7.1	712
2–10b	0.000135	8.2	724
3–7a	0.000682	41.3	883[a]
3–7b	0.001932	116.9	1015[a]
4–8a	0.000092	5.6	692
4–8b	0.000075	4.5	675
4–9a	0.000116	7	710
4–9b	0.000163	9.9	740
6–10a	0.000089	5.4	689
6–10b	0.000064	3.9	664
8–6a	0.000092	5.6	692
8–6b	0.000062	3.8	662

[a] Large cracks present on analytical surface.

cordant Jack Hills zircons, which most likely became discordant at low temperatures. Uranium-lead concordance % versus $\delta^{18}O_{VSMOW}$ zircon data (Table 1 and Table S3) and results from *Cavosie et al.* [2005] are plotted in Figure 3. These data also incorporate some grains that are <3.8 Ga (Table S3). Data were divided into three categories: (1) $\delta^{18}O$ zircon measurements interpreted as magmatic with correlative geochronology; (2) oxygen data (regardless of concordance) where retrospective image studies revealed oxygen measurements were collected on grain cracks; and (3) data which do not overlap cracks, but are from zircon domains ≥10% discordant. The figure shows that more discordant zircons do not tend toward the isotopically heavy O-isotope composition ($\delta^{18}O \geq +10‰$) of the host quartz-pebble conglomerates at the Jack Hills [*Cavosie et al.*, 2005].

[28] The data are not entirely systematic; zircon $\delta^{18}O$ values for two highly discordant grains (JH992CU11_10-8: Figure S1, no. 89; JH992_42: Figure 1, no. 1) deviate from this trend and one of these (JH992CU11_10-8) hosts a visibly metamict domain. This behavior in $\delta^{18}O$ zircon versus U/Pb concordance % has also been observed for measurements of whole zircon splits, where more discordant aliquots tend to have lower $\delta^{18}O$ values [*Bibikova et al.*, 1982; *Valley et al.*, 1994]. A separate study analyzed grains by ion microprobe and reported a similar trend toward lower $\delta^{18}O$ values in zircons with decreasing U/Pb concordance at the scale of tens of micrometers [*Booth et al.*, 2005].

3.3. Jack Hills Zircon Ti Thermometry

[29] Table 3 reports zircon Ti concentrations and corresponding crystallization temperatures for 13 grains; the 25 spot locations are shown in Figure 1 and Figure S1. These results record an average value of 682°C which agrees well with previous Hadean zircon measurements [*Watson and Harrison*, 2005, 2006; *Valley et al.*, 2006]. This average excludes three "temperatures" which were the result of contamination in Ti due to large cracks on the analytical surfaces. This observation provides justification for our rationale to reject oxygen analyses taken on visible cracks. Our multiple Ti concentration measurements allow for intragrain temperature comparisons, which are made on the basis of the internal error associated with counting statistics, not the external error associated with reproducibility of the standard [*Watson et al.*, 2006]. Most replicate analyses are indistinguishable within analytical precision of the CAMECA 3f ion microprobe, indicating general Ti homogeneity among individual grains.

[30] Grain JH0101-2_5-11 (Figure S1, no. 78; ~40% concordant, 3997 Ma) analyzed in triplicate, records temperatures of 588°C, 626°C, and 629°C, outside the range of internal error and reflects the lowest temperatures yet reported for a JH zircon. The two nearly concordant grains with internal temperature differences are JH992CU11_4-9 and JH992CU11_8-6. Grain JH992CU11_4-9 contains 4038 Ga and 4017 Ga geochronology spots correlative with 740°C and 710°C temperatures, respectively. JH992CU11_8-6 records temperatures of 662°C and 692°C. The geochronology spots do not directly overlay these temperature measurements, but the 692°C spot corresponds to a grain region slightly closer to the cathodoluminescent center (Figure 1, no. 55). These results may record the cooling history of these Hadean zircons. In other words, a cooling magma still saturated in zircon would be expected to continue to grow zircon, but with a lower Ti content reflecting the cooler melt conditions. Such intragrain temperature

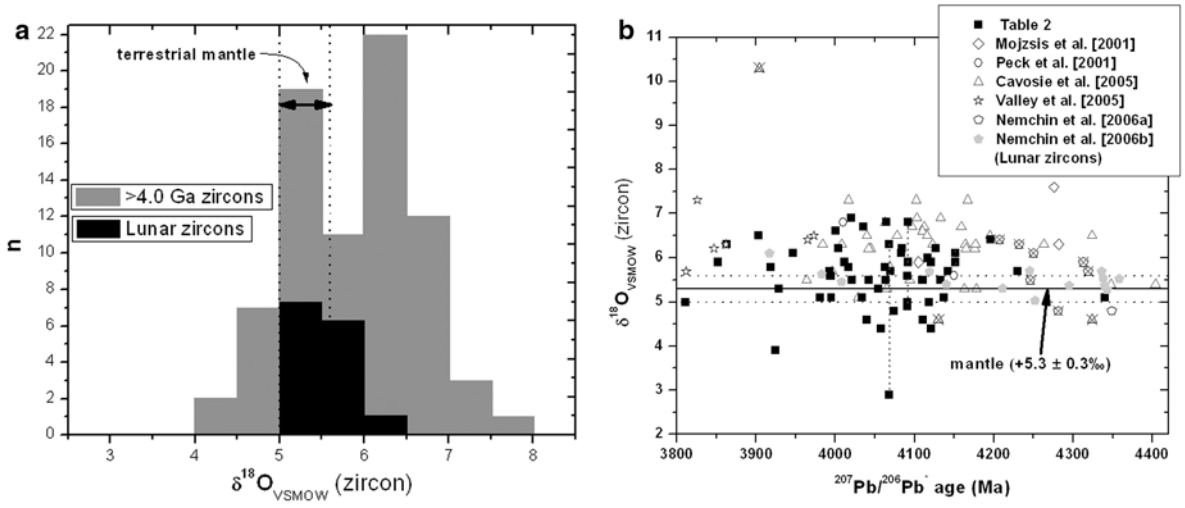

Figure 4. (a) Zircons with ion microprobe U-Pb geochronology ages >4 Ga and correlative $\delta^{18}O_{VSMOW}$ (zircon) measurements. The accepted data reported by respective works are as follows: *Mojzsis et al.* [2001] (n = 3), *Peck et al.* [2001] (n = 2), *Cavosie et al.* [2005] (n = 33), *Nemchin et al.* [2006a] (n = 1), and data from Table 2 (n = 38). Lunar zircon data from *Nemchin et al.* [2006b] in black show that these define a more restricted field of values compared to terrestrial Hadean zircons. (b) Oxygen data plotted versus $^{207}Pb/^{206}Pb$ age for Hadean zircons; error bars have been removed for clarity. The data set is as follows: *Mojzsis et al.* [2001] (n = 3; $1\sigma = \pm 0.3‰$), *Peck et al.* [2001] (n = 2; $1\sigma = \pm 0.8‰$), *Cavosie et al.* [2005] (n = 37; $1\sigma = \pm 0.4‰$), *Nemchin et al.* [2006a] (n = 8; $1\sigma = \pm 0.3‰$), *Valley et al.* [2005] (n = 6; errors not reported), and data from Table 2 (n = 53; $1\sigma = \pm 0.7‰$). *Mojzsis et al.* [2001] reported internal errors; all others are reported as external. Primarily, error differences arise from the standard AS-3 (Table 2) versus 91500 [*Nemchin et al.*, 2006a] versus KIM-5 [*Cavosie et al.*, 2005] and the style of analysis, i.e., monocollection [*Peck et al.*, 2001] versus multicollection [e.g., *Mojzsis et al.*, 2001]. Data accepted by Cavosie are 85% concordant or better; data we report here from Table 2 are 90% concordant or better, after analysis of data presented in Figure 3. Crosses through data points are those rejected by *Cavosie et al.* [2005] and *Nemchin et al.* [2006a] on the basis of "non-magmatic zoning" from their analysis of CL images.

variations were also noted by *Watson and Harrison* [2005].

4. Discussion

4.1. Oxygen Isotopes in Hadean Zircon

[31] A compilation of age-indexed pre-4.0 Ga zircon oxygen data (Table 2) with our new results is presented in Figure 4 [*Mojzsis et al.*, 2001; *Peck et al.*, 2001; *Cavosie et al.*, 2005; *Valley et al.*, 2005; *Nemchin et al.*, 2006b] along with lunar data for comparison [*Nemchin et al.*, 2006a]. The compilation includes only those zircon data accepted by various workers on the basis of separately established criteria regarding what constitutes "primary" oxygen isotope values. It is evident from the data in Figure 4a that the terrestrial Hadean zircon oxygen isotope distribution contains a peak offset from mantle zircon by about +1‰ and that these values extend well beyond the highest measured lunar zircon oxygen isotopes (Figure 4a). This observation argues against a scenario in which Hadean zircons were exclusively derived from protoliths in equilibrium with the mantle, or that they formed in some process that could only have been common to the Earth and Moon. The probability of identical populations viz. Kolmogorov-Smirnov (section 3.1) is <5% for the $\delta^{18}O$ zircon distribution in Table 2, in comparison with lunar zircon results reported by *Nemchin et al.* [2006b].

[32] Zircon oxygen analyses results considered in equilibrium with the mantle total 26 (5.3 ± 0.3‰), while we find that 24 are above mantle values, and 7 are below +5.0‰. This observation is supported by another Hadean oxygen isotope data set where there is some evidence of oxygen isotope bimodality [*Cavosie et al.*, 2005]. Elevated $\delta^{18}O$ compositions of Hadean zircons further support the hypothesis that zircon source-melts may have interacted with liquid water at or near Earth's surface in the Hadean [*Mojzsis et al.*, 2001; *Peck et al.*, 2001; *Wilde et al.*, 2001; *Valley et al.*, 2002; *Cavosie et al.*, 2005]. If this interpretation is correct, it is worth exploring whether stable liquid

water persisted at Earth's surface for much or all of the Hadean. This expanded data set coupled with other separate lines of evidence (sections 4.3 and 4.5) suggests that some of the Hadean source melt precursors were in chemical communication at or near the surface of the Earth.

[33] When all available Hadean $\delta^{18}O$ zircon results are plotted versus $^{207}Pb/^{206}Pb$ zircon age (Figure 4b) it is apparent that data are sparse for both the 4.4–4.2 Ga and 3.95–3.85 Ga time intervals. Secular changes in $\delta^{18}O$ zircon values from 4.4 Ga to 4150 Ma [*Cavosie et al.*, 2005] need to be verified with more data, but available records seem to indicate water-rock interaction (and thus enriched $\delta^{18}O$ zircon values) as early as 4.3–4.2 Ga. Progressively more positive and negative ε_{Hf} values as a function of time in Hadean zircons have been interpreted to show that substantial continental crust formation began at 4.4–4.5 Ga [*Harrison et al.*, 2005a, 2006; cf. *Valley et al.*, 2006]. A consequence of the (rapid?) early increase in the volume of continental crust would be subsequent increases in the volume of recycled supracrustal rocks, which in turn could have led to Hadean melts that crystallized zircons with more elevated $^{18}O/^{16}O$ values.

[34] Is a decrease in $\delta^{18}O$ zircon values at 3.95 Ga and after (Figure 4b) preserved? On the basis of the secular Hf isotopic evolution observed for the Hadean, *Harrison et al.* [2005a] postulated that massive remixing of Hadean crust back into the mantle must have occurred because large (±200) ε_{Hf} values are not preserved on the contemporary Earth [*Vervoort and Blichert-Toft*, 1999]. Under this scenario, any enriched ^{18}O crust signature would become diluted when mixed back into the mantle. *Amelin* [2005] proposed that the onset of the Late Heavy Bombardment could have facilitated the return of crust to the mantle. Again, due to the relatively small number of 3.95–3.8 Ga zircons analyzed, more combined oxygen and Hf isotopic work [*Kemp et al.*, 2006] could either bolster or refute this model.

[35] Two Hadean zircons (JH0101-1_9-20 and ANU32_11-5) preserved $\delta^{18}O$ zircon compositions well below mantle values (Figure 4a). Grain JH0101-1_9-20 (3925 Ma) has a value of +3.9‰ (Figure 1, no. 43). This zircon shows subdued CL zoning in its core region, but retains a high-luminescent rim; all data derived from zircons of this type were rejected by *Cavosie et al.* [2005] because they failed to fit their criterion for well-defined concentric zoning in CL. Two other (rejected) oxygen spots on the same grain yielded +3.6‰, and a near-rim value of 5.5‰. Results for grain ANU32_11-5 are puzzling since two measurements made on top of each other yield very different oxygen isotope compositions (+2.9‰ versus +6.3‰). One analytical aspect of concern is the +2.9‰ measurement shows a ~15% decrease in ^{16}O and ^{18}O counts relative to other measurements where signals were generally reproducible to within ~5%. In BSE, or reflected light images, there is nothing unusual about these grains and no cracks or irregularities exist in the vicinity of the analysis (Figure 1, no. 27). Minute inclusions in zircon could impart oxygen heterogeneity, but it is also not out of the realm of possibility that these zircons record a process in the Hadean crust capable of imparting ^{16}O-rich oxygen (relative to mantle) to zircon domains. Low and even negative $\delta^{18}O$ whole rock values are sometimes present where large meteoric convective hydrothermal systems have been established [*Taylor and Sheppard*, 1986]. These hydrothermally altered rocks can then be remelted to form low $\delta^{18}O$ magmatic zircons [e.g., *Bindeman and Valley*, 2001].

4.2. Preservation of Primary $\delta^{18}O$ Values in Hadean Zircons

[36] To evaluate whether measured oxygen isotope ratios reflect their crystallization environment requires an understanding of oxygen retention in zircon, and knowledge of the geologic history of Hadean zircons. We review some empirical and experimental results for oxygen retention in zircon, and discuss the likelihood of primary oxygen preservation, given current understanding of predepositional and postdepositional histories of these grains.

[37] Coherent zircon crystal cores, interpreted as such from their oscillatory cathodoluminescence (CL) patterns, have been interpreted to retain oxygen isotope compositions through a variety of metamorphic regimes. *Valley et al.* [1994] have argued that original $\delta^{18}O$ zircon at time of formation is preserved through amphibolite to granulite facies metamorphic conditions. Differences in zircon core-rim $\delta^{18}O$ values of as much as 5.6‰ have been documented for Grenvillian zircons [*Peck et al.*, 2003], and non-metamict "pristine" zircon has been shown to be resistant to hydrothermal alteration and oxygen isotope exchange at least at the biotite grade [e.g., *King et al.*, 1997]. Diffusion of oxygen in zircon has been explored experimentally under dry ($P_{H2O} \sim 7$ MPa) and wet ($P_{H2O} \geq 7$ MPa) conditions [*Watson and Cherniak*, 1997]. Results

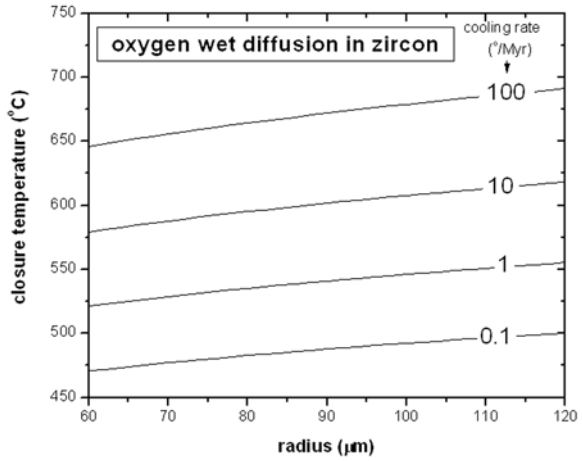

Figure 5. Bulk closure temperatures for oxygen diffusion in zircon, as a function of relevant zircon crystal radii (60–120 μm), under different cooling rates. Results were calculated using the Arrhenius relationship for wet oxygen diffusion in zircon [*Watson and Cherniak*, 1997].

show that a zircon with a 100 μm effective diffusion radius can retain core δ^{18}O values at 900°C for 65 Ma under dry conditions (applicable to granulite grade metamorphism), but under wet conditions, closure temperatures for oxygen isotopes are ~650°C for a cooling rate of 100°C/Ma and a diffusion radius of ~80 μm [*Watson and Cherniak*, 1997]. In general, empirical observations and experiment broadly agree that oxygen in zircon is extremely retentive under dry conditions and that it can be preserved under wet conditions, but probably not at temperatures much above ~600°C.

[38] The circa 3.1 Ga postdepositional history of sediments hosting Hadean zircons is not especially well constrained; the only known widespread event was a 2.7 Ga upper greenschist to lower amphibolite facies metamorphism [e.g., *Pidgeon and Wilde*, 1998]. The JH metasediments are mature (90–100% SiO_2), and quartz clasts have δ^{18}O values of +10–12‰ [*Cavosie et al.*, 2005], as much as 7‰ higher than Hadean JH zircons. Some insight into oxygen isotope exchange can be obtained from Figure 3.

[39] If the current degree of observed discordance results from low temperature Pb* loss (i.e., metamictization), it is conceivable that grains which are discordant today were either equally or more susceptible to oxygen exchange during the 2.7 Ga metamorphic event cited above. This logic is based on the premise that grains which are metamict and discordant today (most likely because of high U and Th contents), would have been more likely to be structurally damaged prior to the last known widespread regional metamorphism. The fact that these equally or more susceptible grains do not trend toward host sediment values suggests that substantial ^{18}O enrichment did not occur in more pristine (>90% concordant) zircons presented in Table 2. This analysis relies on evidence that is somewhat tenuous, and without proper oxygen diffusion profiles for these Hadean zircons, arguments for and against diffusive oxygen exchange cannot be evaluated further. However, zircons with short diffusion radii (<50 μm; approximated by analysis location in grain cross sections) contain mantle δ^{18}O values (e.g., Figure 1, no. 11, 47, 48, 55). This is not the expected result if the zircons underwent substantial exchange with their host sediments.

[40] Knowledge of the history of oxygen isotope exchange in Hadean zircons is fundamentally hampered by their unknown histories prior to deposition (>3.1 Ga). Four Hadean zircons investigated by high resolution ion microprobe depth profiles [*Trail et al.*, 2007] preserve early Archean overgrowths and/or modifications of Hadean cores. Ages less than or equal to 3.9 Ga represent ~10–15% of the total grain radius (typically 60–80 μm). The presence of overgrowths or alteration zones on older preexisting zircon cores opens the possibility that diffusive exchange of oxygen may occurred. Closure temperatures for oxygen in zircon as a function of crystal radii most applicable to Jack Hills grain size distributions are shown in Figure 5. Provided our interpretation of the metamorphic history of the Jack Hills zircons is correct [*Trail et al.*, 2007], we consider predepositional oxygen diffusion the most plausible scenario for oxygen contamination of Hadean zircons.

4.3. Ti-in-Zircon Thermometry

[41] Hadean zircons enriched in heavy oxygen were used to argue for crust in chemical communication with surface environments. The addition of water to the zircon source melts will lower the eutectic leading to low temperature melts. Calibration of the $[Ti]_{zircon}$ thermometer [*Watson and Harrison*, 2005; *Watson et al.*, 2006] places unique quantitative constraints on zircon crystallization temperatures. Our new results reflect temperatures which are consistent with minimum-melting granitoid-type conditions reported by *Watson and Harrison* [2005] and agree with other recent Hadean zircon thermometry measurements [*Watson and Harrison*,

2006; *Valley et al.*, 2006]. In addition, knowledge of $\delta^{18}O$ and crystallization temperature provides enough information to make indirect calculations of $\delta^{18}O$ values of other minerals present in the host rocks. For example, empirical calculations performed by *Valley et al.* [2003] show that crystallization of zircon with $\delta^{18}O$ = +6.0–6.5‰, at the temperatures of ~680–700°C predicted by *Watson and Harrison* [2005], would co-exist with quartz at ~+9.0‰. This value is also consistent with the O-isotope composition of quartz in many granitic rocks [*Taylor*, 1968].

[42] The lowest $[Ti]_{zircon}$ measurement documented in this study was on a ~40% concordant grain, with a Ti concentration that corresponds to temperatures as low as 588°C (Figure S1, no. 78) and consistent with a sub-solidus origin. However, since this grain shows evidence for substantial Pb loss, lower Ti concentrations could also reflect pervasive grain alteration. It is possible to estimate Ti diffusion for pristine zircon grains on the basis of the relatively systematic diffusion behavior observed for tetravalent cations in the zircon structure as a function of ionic radius [*Cherniak et al.*, 1997]. On the basis of this analysis, only temperatures in excess of 1100°C are likely to lead to Ti diffusion in zircon over the diffusion length scales typical in Jack Hills zircons. This calculation agrees well with the recently derived Arrhenius equation from completed Ti diffusion experiments in zircon [*Cherniak and Watson*, 2006]. While there is no way to explicitly test for Ti diffusion, this zircon has a Th/U ratio of 3.2 that may be indicative of mobilization of U [*Cavosie et al.*, 2004]. Since Ti diffuses at slightly lower temperatures than U, it may have been mobilized and the low Ti-derived temperature record may be invalid.

4.4. Using Ti-in-Zircon Thermometry as a Protolith Discriminator

[43] Alternative views have been presented which argue that the Ti thermometer cannot be used to constrain zircon provenance [*Fu et al.*, 2005; *Kamber et al.*, 2005; *Nutman*, 2006; *Glikson*, 2006; *Valley et al.*, 2006; *Coogan and Hinton*, 2006]. A criticism common to these reports is the concern over uncertainties in Zr and Ti activities in Hadean zircon source melts. For example, a late stage mafic melt may saturate the residual at low temperatures in Zr (and Si), to subsequently crystallize zircon. It was proposed that zircon crystallization temperatures could not be used to uniquely separate this process (or an analogous process) from granitic, water-saturated minimum melt conditions [*Valley et al.*, 2006; *Coogan and Hinton*, 2006]. However, the current Ti data suggests that the majority of zircons that crystallized from mafic sources (including late-stage residuals) are different in peak and distribution [*Watson et al.*, 2006; *Valley et al.*, 2006] than Hadean zircons, which argues against a common origin [*Harrison et al.*, 2006, 2007; *Watson and Harrison*, 2006]. It was also suggested that tonalites could crystallize zircons at temperatures indistinguishable from minimum melt conditions implied for the Hadean source rocks [*Nutman*, 2006]. This possibility for the majority of Hadean zircon is ruled out because saturation temperatures in tonalitic melts are demonstrably higher than the 680 ± 25°C peak observed for Hadean zircons [*Harrison et al.*, 2006]. Finally, it was recently shown by calculation and geologic example that igneous rocks formed at higher temperatures (>750°C) produce Ti-derived temperatures well above the wet granite solidus [*Harrison et al.*, 2007]. However, a minor component (<10%) of the Hadean zircons thus far analyzed could have been derived from a TTG-type melt on the basis of ~750°C crystallization temperatures in some grains.

[44] The Ti thermometer applies directly to systems which contain a pure TiO_2 phase (e.g., rutile), but suitably to melts with a Ti-saturated phase (e.g., ilmenite). Since Ti-activity is not strictly quantified in JH source melts, it was argued that measured temperatures could reflect Ti melt activity <1 rather than granitic minimum melt conditions [*Nutman*, 2006; *Coogan and Hinton*, 2006]. However, melts that contain high activities of Zr required for zircon saturation generally contain high activities of Ti. Ti-activity in melts has been characterized for magmas of diverse compositions [*Ryerson and Watson*, 1987], and more recently among siliceous melts such as trondjhemite, s-type granite, and metaluminous granite [*Hayden et al.*, 2005]. Results have shown that a siliceous melt, independent of water content, will often saturate in a Ti bearing phase before zircon [*Ryerson and Watson*, 1987; *Hayden et al.*, 2005]. This reasoning relies on the expectation that Hadean zircon source melts have SiO_2 activity of ~1. This is substantiated because many SiO_2 inclusions have been discovered in all Hadean zircon inclusion studies to date [*Maas et al.*, 1992; *Peck et al.*, 2001; *Trail et al.*, 2004; *Cavosie et al.*, 2004; *Crowley et al.*, 2005]. It is worth noting though that melts with low Si-activity would only serve to compensate for sub-unity Ti activity [*Ferry and Watson*, 2007].

[45] Data have been shifted to show the effect of sub-unity Ti activity in the initial publication presenting the thermometer [*Watson and Harrison*, 2005] and more recently by *Coogan and Hinton* [2006] during their comparison of 15 zircons from five oceanic gabbros. Figure 1 of *Coogan and Hinton* [2006] demonstrates that direct comparison of the two populations shows they are dissimilar. *Coogan and Hinton* [2006] drew an arrow in their Figure 1 to show the shift in crystallization temperatures for Hadean zircons if the source melts had Ti activity of 0.5, perhaps to imply a similar distribution with their temperature data. We disagree with this comparison because all five gabbros in their study crystallized in the presence of ilmenite, which implies sub-unity Ti-activity, so that a sub-unity shift must be applied the data of *Coogan and Hinton* [2006] as well. Studies that have explored zircon crystallization in the presence of ilmenite have previously yielded Ti-activities of ~0.6 [*Watson et al.*, 2006]. The uncertainties of the Ti thermometer when applied to zircons of unknown origin can be reasonably constrained, and it remains clear that results that bear on conditions of Hadean zircon crystallization are reproducible [*Watson and Harrison*, 2006].

4.5. Hadean Zircon Rare Earth Element Partitioning

[46] It has generally been assumed that Hadean zircons are magmatic, a basis for the interpretation of our data. Here, we apply the lattice strain theory of partitioning to rare earth elements (REEs) in zircon, a model which is intended for application to crystal-melt partitioning [*Blundy and Wood*, 1994]. In other words, REEs of metamorphic (or hydrothermal) zircon are expected to show deviations from the parabolic behavior of partition coefficients versus ion radii of substituent ions, if partition coefficients are calculated from magmatic compositions. In this section, we show that the lattice strain model can help distinguish magmatic from metamorphic/hydrothermal zircons, and conclude that Hadean zircons are dominantly magmatic (sections 4.5.1 and 4.5.2). We further discuss whether REE patterns of Hadean zircons can be employed for provenance determinations (section 4.5.3).

[47] To achieve this, we have compiled 73 published REE concentrations from 51 Hadean zircons [*Maas et al.*, 1992; *Wilde et al.*, 2001; *Peck et al.*, 2001; *Crowley et al.*, 2005]. In an attempt to match zircon provenance, various generic whole rock REE compositions of magmatic origin were used to approximate REE melt concentrations, and to calculate hypothetical REE zircon partition coefficients. The model compositions chosen for this analysis, from felsic to more mafic were: Archean granite [*Condie*, 1993], Archean tonalite-trondhjemite-granodiorite [*Condie*, 1993], adakite [*Samsonov et al.*, 2005], anorthosite [*Markl*, 2001] and N-type MORB [*Sun and McDonough*, 1989]. The lattice strain equation was then fit to the five sets of partition coefficients for each of the 73 REE measurements, assuming average T = 680°C for Hadean zircons. In this calculation, r_o = 0.84 Å, D_o and E are free parameters and were allowed to vary during curve fitting. The best-fit among the candidate rock types was determined simply by comparing the R^2 values. It is worth noting that changing the crystallization temperature will not change the R^2 value of a fit, but will change E.

[48] We have evaluated this approach by selecting zircons from a variety of host rocks of known provenance, including rock types which were not included in our five model compositions [*Hoskin*, 1998, 2005; *Hoskin and Black*, 2000; *Hoskin and Ireland*, 2000; *Dawson et al.*, 2001; *Rubatto*, 2002; *Whitehouse and Platt*, 2003; *Whitehouse and Kamber*, 2003, 2005; *Pettke et al.*, 2005]. In this way, 68 magmatic, 47 metamorphic, and 24 "hydrothermal" published zircon REE data were fit to the lattice strain model using our five host rock types (Table S4).

4.5.1. Magmatic Versus Metamorphic Zircon

[49] The usefulness of CL images as a guide for selecting ion microprobe analysis spots was demonstrated by correlation of zones typically interpreted as magmatic with elevated $\delta^{18}O$ zircon spots [*Cavosie et al.*, 2005]. Although cathodoluminescence images are informative, interpretations can be subjective and the suite of textures inferred to be magmatic versus metamorphic can be ambiguous [*Corfu et al.*, 2003]. Because of this ambiguity, *Cavosie et al.* [2005] and *Nemchin et al.* [2006a] chose to err on the side of caution and reject from consideration Hadean zircons which do not contain characteristic magmatic zoning as deduced from CL images.

[50] Derived REE partition coefficients for igneous versus metamorphic zircon show a definite quantifiable difference between the two. Our application of the lattice-strain model shows that the average best-fit R^2 value for 68 igneous zircons is 0.89 ±

0.07 (1σ). This is in contrast to our analysis of 47 metamorphic zircons (or metamorphic grain regions) which have an average best-fit R^2 value of 0.67 ± 0.15. The results provide a baseline for comparison to Hadean zircons, which have an average best-fit R^2 value of 0.88 ± 0.06, highly suggestive of an igneous origin. As a visual example, Figure 6a shows the lattice strain function curves fit to the five partition coefficient sets for a Jack Hills zircon, to show the parabolic behavior common among the 68 igneous test cases. For comparison, representative partition coefficient sets from the five attempted host rocks fits are shown for a metamorphic zircon from the granulite-grade garnet gneiss near the Carratraca peridotite massif (Figure 6b). Partition coefficients versus ion radii for the metamorphic grain region shows deviations from predicted magmatic partitioning (compare to Figure 6a). This example, along with others, suggests that (hypothetical) partition coefficients of metamorphic zircons calculated from igneous host rocks are unlikely to mimic the parabolic behavior seen for magmatic zircon-melt partitioning [e.g., *Manning et al.*, 2006]. We find in our analysis that Hadean zircons (with very few exceptions; see section 4.5.2) are reconcilable with a magmatic origin. A noteworthy feature of some metamorphic zircons is that they show flat partitioning of HREEs, a common feature of zircons which crystallized in the presence of garnet [e.g., *Whitehouse and Platt*, 2003; *Rubatto*, 2002]. This type of partitioning is not present in Hadean zircons which would seem to indicate that the grains did not form in the presence of garnet.

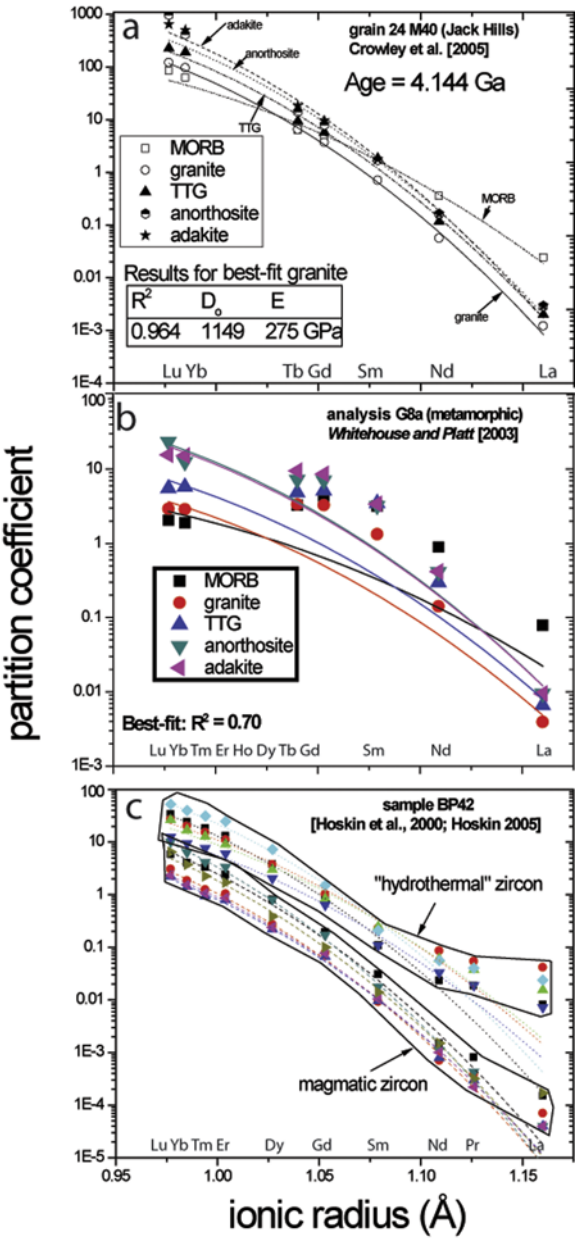

Figure 6. (a) Partition coefficient sets versus ionic radius (Å) for different host rock candidates of a representative Hadean zircon. We used the *Blundy and Wood* [1994] lattice strain model and a crystallization temperature of 680°C [*Watson and Harrison*, 2006], and best host rock fit was resolved by the R^2 value. In this particular grain from *Crowley et al.* [2005], the best fit was Archean granite [*Condie*, 1993]. (b) Representative REE partition coefficients for our five host rocks calculated for a metamorphic grain region [*Whitehouse and Platt*, 2003]. This metamorphic grain region, like others (Table S4), shows that partition coefficients derived from igneous rocks deviate from the lattice strain model. The color-correlated lines correspond to attempted fits to the partition coefficients. (c) Trace element partition coefficients of magmatic and hydrothermal zircon from aplite sample BP42 [*Hoskin*, 2005]. Hydrothermal zircons show REE deviation in partition coefficients relative to magmatic zircons, most noticeable in La, Pr, and Nd. In this particular case, our five host rocks were not used because whole rock concentrations were available from *Hoskin et al.* [2000]. The lattice strain model has an average magmatic fit of R^2 = 0.89 (n = 5) and a hydrothermal fit of R^2 = 0.76 (n = 5).

4.5.2. Hydrothermal Modification of Hadean Zircon

[51] *Hoskin* [2005] proposed that metamict zones of Hadean zircons could have been enriched in heavy oxygen and LREE during postprimary crystallization by hydrothermal fluids. Despite crystallization ages that were indistinguishable in different domains of complex zircons, that study found high concentrations of LREE in "hydrothermal" mantles relative to igneous cores in zircons from the Boggy Plain zoned pluton in eastern

Australia. The preferred model for these features was that later fluids imparted high $^{18}O/^{16}O$ ratios to the zircons and were responsible for the enriched LREE patterns as well. In this scenario, plate boundary processes would be unnecessary to account for high $\delta^{18}O$ zircon values in the Hadean [*Hoskin*, 2005]. Experimental work supports this proposal since hydrothermal annealing of metamict zircon is possible at 350°C or lower [e.g., *Geisler et al.*, 2003].

[52] At the time when the *Hoskin* [2005] manuscript was submitted (Dec. 2003), only one CL image of a Jack Hills zircon with ion microprobe oxygen spots [*Wilde et al.*, 2001; *Peck et al.*, 2001] and two other Hadean zircon images [*Nelson et al.*, 2000] were published. Therefore conclusions that supported a hydrothermal origin for altered Hadean zircons arose on the basis of a few CL images as well as high $\delta^{18}O$ values (+10‰) for one (discordant) zircon core [*Mojzsis et al.*, 2001]. There now exists a large data set of published Hadean zircon CL images [*Cavosie et al.*, 2004, 2005; *Dunn et al.*, 2005; *Crowley et al.*, 2005] (Figures 1 and S1), many of which display concentric zoning usually ascribed to a magmatic origin [*Cavosie et al.*, 2004]. Some zircons with concentric zones record $\delta^{18}O$ zircon well above mantle values, which do not appear to lend support to the annealing hypothesis as an important process for ^{18}O enrichment in these grains. Other studies have shown that hydrothermal zircons (or hydrothermally altered regions) are frequently enriched in Hf, usually by $\geq$2% [e.g., *Kerrich and King*, 1993; *Hoskin*, 2005]. Out of 135 analyses which specifically characterized Hadean zircons for Hf [*Maas et al.*, 1992; *Cavosie et al.*, 2005; *Crowley et al.*, 2005] average concentrations are 0.94% (range = 0.66–1.4%).

[53] We sought to evaluate whether the lattice strain model can be used to distinguish between igneous zircon and zircon grain regions annealed by hydrothermal fluids. Rare earth element partition coefficients were fit to the lattice strain function in the same manner discussed above for 24 hydrothermal zircons [*Hoskin*, 2005; *Pettke et al.*, 2005]. Results show hydrothermal zircons have a best-fit R^2 average of 0.78 ± 0.05. For comparison, Figure 6c shows hydrothermal and igneous zircons from sample BP42 [*Hoskin*, 2005; *Hoskin et al.*, 2000]. It is evident that hydrothermal zircon shows large partition coefficient deviations compared to magmatic zircon, a phenomenon seen in only 3 of 73 Hadean zircon REE analyses explored here (i.e., R^2 <0.78; see Tables S4 and S5 and compare with recent results of *Cavosie et al.* [2006]). With few exceptions, calculated REE partition coefficients in Hadean zircons do not to deviate from the lattice strain model. Unless the assumptions of the lattice strain model have been violated, we can conclude that the majority of Hadean zircons with LREE-enriched concentrations, likely preserve a signature from their primary magmatic values.

[54] To summarize, in concert with the Ti data [*Watson and Harrison*, 2005] and image analysis [e.g., *Cavosie et al.*, 2004], we have found that the vast majority (~95%) of Hadean zircons are magmatic. However, we are not confident that we can unambiguously distinguish between metamorphic versus hydrothermal zircon solely on the basis of the above analysis.

4.5.3. Provenance Discrimination

[55] *Maas et al.* [1992] demonstrated that REE concentrations in Hadean zircons show marked enrichment in LREE, similar to zircon compositions from Phanerozoic diorites and granites. Follow-up $\delta^{18}O$ zircon measurements along with REE studies of JH zircons by *Wilde et al.* [2001] and *Peck et al.* [2001] showed that correlative high $\delta^{18}O$ zircon values with enriched LREEs appear consistent with zircons derived from granitoid-type source rocks. In another study, trace element patterns and U concentrations of Hadean and early Archean detrital zircons from Mount Narryer were used to argue that the MN grains were derived from evolved granitic rocks, but that the JH zircons are not [*Crowley et al.*, 2005].

[56] *Whitehouse and Kamber* [2002] challenged these interpretations on the basis of their analysis of circa 3.81 Ga zircons from a West Greenland orthogneiss sample. In their study, it was assumed that the rock was pristine and that whole rock REE values reliably reflect magmatic REE abundances at time of emplacement. Because LREE abundances measured in the whole rock and the zircons appeared to be inconsistent with predicted partition coefficients for zircon-melt, *Whitehouse and Kamber* [2002] concluded that models which derive source melt characteristics from zircon alone are not reliable.

[57] To explore this further, Figure 6a illustrates the variability in partition coefficients depending on different model melt compositions for a selected Hadean zircon. In this specific case, best-fit results for the lattice-strain parabola according to *Blundy and Wood* [1994] favor a granitic protolith. Of the 70 published Hadean zircon REE patterns inter-

preted as magmatic (i.e., excluding the 3 with $R^2<0.78$), we found 26 best-fits for granite, 24 for tonalite-trondhjemite-granodiorites, 7 for adakite, 1 for anorthosite, and 12 for N-type MORB (Table S4). This calculation seems appealing at first because a significant population of zircons indicate REE partitioning consistent with crystallization from a granitoid-type melt. However, during our investigation, we found the lattice-strain theory sometimes predicts protolith REE compositions for zircons of known provenance that are better fits with rocks for a different lithology.

[58] For example, 6 zircons from two separate felsic metagranitoids [*Hoskin and Black*, 2000] predicted granite (4×), TTG (1×), adakite (1×) as the host rocks. In another case, zircons analyzed from a quartz diorite [*Whitehouse and Kamber*, 2003] produced granite (6×), TTG (5×), MORB (1×), and adakite (1×) as the host rock solutions. The MADRID zircon taken from an ultramafic rock ascribed a kimberlitic origin [*Hoskin*, 1998; *Dawson et al.*, 2001] predicted host rocks of adakite (3×), anorthosite (3×), and TTG (1×). The last result broadly supports our model because no kimberlitic rock was included in our host rock matches, yet appropriately, the model still generally predicted a mafic rather than felsic end-member. An analogous result was achieved for a harzburgite xenolith [*Dawson et al.*, 2001] which returned best fits for an anorthosite host rock for all 17 zircons.

[59] Since the partition model sometimes predicts rocks that the zircons did not form in, we cannot be confident about specific assignment of a protolith based exclusively on this model. However, if we generalize our five rock-types into felsic (granite and TTG) versus mafic (adakite, anorthosite, MORB) for zircons of known provenance, then the zircon parentage is correctly classified ~80% of the time. Given these results, we can propose that REE partitioning indicates a felsic (n = 50) rather than a mafic (n = 20) end-member for the majority of Hadean zircons thus far studied. The results of section 4.5.3 should be considered a qualitative guide that lends support to other more quantitative lines (O-isotopes, Ti, mineral inclusions) for a dominantly granitic rather than mafic origin of most Hadean zircons.

5. Summary

[60] Of the δ^{18}O zircon measurements reported here on 89 pre-3.8 Ga zircons, 50 of these grains were free of analytical artifacts resulting from cracks, correlatable by CL with geochronology spots, and ≥90% concordant. Of these 50 grains, 15 analyses contained δ^{18}O values out of equilibrium with a pure mantle source end-member (≥6.0‰), five of which were above +6.5‰. In agreement with previous results [e.g., *Mojzsis et al.*, 2001; *Peck et al.*, 2001; *Cavosie et al.*, 2005] we find that approximately 25% of pre-3.8 Ga grains so far analyzed preserve resolvable ^{18}O enrichments above mantle equilibrium values. We analyzed a number of variably concordant zircons to search from trends in δ^{18}O zircon and U/Pb % concordance and found that counter to expectation, more discordant zircons do not tend toward average sediment values of +10–12‰.

[61] Independently, our Ti measurements on selected zircons reflect crystallization temperatures consistent with the hypothesis that most Hadean zircons were sourced from low temperature, minimum melt conditions. Such conditions are best satisfied by water-saturated granitoid-type sources [*Watson and Harrison*, 2005, 2006; *Harrison et al.*, 2007]. The one exception provided temperatures which ranged from 588–629°C. This is the lowest temperature recorded for Hadean zircon thus far, and while the discordant nature of the grain calls into question the validity of using Ti concentration to reflect on the true crystallization temperature, the result is consistent with our REE analysis which indicated very small component of Hadean zircon source rocks are not of igneous origin.

[62] In addition, we have evaluated scenarios which have been presented as alternatives to the granite theory of Hadean zircon petrogenesis [e.g., *Whitehouse and Kamber*, 2002; *Hoskin*, 2005]. These studies based their conclusions on analysis of REE in zircon from specific case examples, and to follow-up on that work we have compiled REE data from Hadean zircons in an attempt to match these to various host lithotypes using the *Blundy and Wood* [1994] lattice-strain model. We find that (1) there is broad support for view that Hadean zircons are dominantly of felsic provenance; (2) the partitioning of REE constrains Hadean zircons as being almost entirely (>95%) magmatic; and (3) hydrothermal modification of Hadean zircon (leading to high δ^{18}O zircon and enriched LREE) is rare or absent in the samples thus far described.

[63] We conclude, on the basis of the several lines of evidence discussed above, that unless that Hadean Earth operated in a manner fundamentally different from all that we know, the simplest

explanation for all observed data is that an evolved rock cycle that included the pervasive activity of liquid water in the context of formation of granitic crust was present on Earth by 4.3–4.2 Ga.

Acknowledgments

[64] Support from the NASA Exobiology Program (NAG5-13497) "Mission to Really Early Earth" to S.J.M., the NASA Astrobiology Institute, the NSF Instrumentation and Facilities Program and Australian Research Council to T.M.H., and NSF grant EAR-0440228 to E.B.W. are greatly appreciated. D.T. gratefully acknowledges fellowship support from the Alfred P. Sloan Foundation. The ion microprobe facility at UCLA is partly supported by a grant from the Instrumentation and Facilities Program, Division of Earth Sciences, National Science Foundation. O. M. Lovera (UCLA) provided assistance with Kolmogorov-Smirnov calculations. G. B. Morgan and D. London (OU) are thanked for assistance with CL imaging. N. L. Cates assisted with data collection. The unpublished Ti diffusion data for zircon made available by D. J. Cherniak are much appreciated. This manuscript benefited from discussion with E. J. Catlos, A. J. Cavosie, and P. Holden, the constructive and very thorough comments of three anonymous reviewers, and helpful suggestions from the handling editor, V. J. M. Salters.

References

Amelin, Y. (2005), A tale of early Earth told in zircons, *Science*, *310*, 1914–1915.

Benninghoven, A., F. G. Rüdenauer, and H. W. Werner (1987), *Secondary Ion Mass Spectrometry: Basic Concepts, Instrumental Aspects, Applications and Trends*, 1227 pp., John Wiley, Hoboken, N. J.

Bibikova, Y. V., V. I. Ustinov, T. V. Gracheva, M. A. Kiselevskiy, and Y. A. Shukolyukov (1982), Variations of isotopic composition of oxygen in accessory zircons, *Dokl. Akad. Nauk SSSR*, *264*, 698–700.

Bindeman, I. N., and J. W. Valley (2001), Low-δ^{18}O rhyolites from Yellowstone: Magmatic evolution based on analyses of zircons and individual phenocrysts, *J. Petrol.*, *42*, 1491–1517.

Black, L. P., et al. (2004), Improved ^{206}Pb/^{238}U microprobe geochronology by the monitoring of a trace-element-related matrix effect; SHRIMP, ID-TIMS, ELA-ICP-MS and oxygen isotope documentation for a series of zircon standards, *Chem. Geol.*, *205*, 115–140.

Bleeker, W. (2004), Towards a "natural" time scale for the Precambrian: A proposal, *Lethaia*, *37*, 219–222.

Blundy, J., and B. Wood (1994), Prediction of crystal-melt partition coefficients for elastic moduli, *Nature*, *372*, 452–454.

Booth, A. L., Y. Kolodny, C. P. Chamberlain, M. McWilliams, A. K. Schmitt, and J. Wooden (2005), Oxygen isotopic composition and U-Pb discordance in zircon, *Geochim. Cosmochim. Acta*, *69*, 4895–4905.

Bowring, S. A., and I. S. Williams (1999), Priscoan (4.00–4.03 Ga) orthogneisses from northwestern Canada, *Contrib. Mineral. Petrol.*, *134*, 3–16.

Caro, G., V. C. Bennett, B. Bourdon, T. M. Harrison, and S. J. Mojzsis (2006), The ^{142}Nd record of Hadean zircons (abstract), *Geochim. Cosmochim. Acta.*, *70*, A85.

Cates, N. L., and S. J. Mojzsis (2006), Chemical and isotopic evidence for widespread Eoarchean (≥3750 Ma) metasedimentary enclaves in southern West Greenland, *Geochim. Cosmochim. Acta*, *70*, 4229–4257.

Cavosie, A. J., S. A. Wilde, D. Y. Liu, P. W. Weiblen, and J. W. Valley (2004), Internal zoning and U-Th-Pb chemistry of Jack Hills detrital zircons: A mineral record of early Archean to Mesoproterozoic (4348–1576 Ma) magmatism, *Precambrian Res.*, *135*, 251–279.

Cavosie, A. J., J. W. Valley, S. A. Wilde, and Edinburg Ion Microphone Facility (2005), Magmatic δ^{18}O in 4400–3900 Ma detrital zircons: A record of the alteration and recycling of crust in the early Archean, *Earth Planet. Sci. Lett.*, *235*, 663–681.

Cavosie, A. J., J. W. Valley, S. A. Wilde, and Edinburgh Ion Microprobe Facility (2006), Correlated microanalysis of zircon: Trace element, δ^{18}O, and U-TH-Pb isotopic constraints on the igneous origin of complex 3900 Ma detrital grains, *Geochim. Cosmochim. Acta*, *69*, 637–648.

Cherniak, D. J., and E. B. Watson (2000), Pb diffusion in zircon, *Chem. Geol.*, *172*, 5–24.

Cherniak, D. J., and E. B. Watson (2006), Ti diffusion in zircon, *Eos Trans. AGU*, *87*(52), Fall Meet. Suppl., Abstract V31F-02.

Cherniak, D. J., J. M. Hanchar, and E. B. Watson (1997), Diffusion of tetravalent cations in zircon, *Contrib. Mineral. Petrol.*, *127*, 383–390.

Compston, W., and R. T. Pidgeon (1986), Jack Hills, evidence of more very old detrital zircons in Western Australia, *Nature*, *321*, 766–769.

Condie, K. C. (1993), Chemical composition and evolution of the upper continental crust: Contrasting results form surface samples and shales, *Chem. Geol.*, *104*, 1–37.

Coogan, L. A., and R. W. Hinton (2006), Do trace element compositions of detrital zircons require Hadean continental crust?, *Geology*, *34*, 633–636.

Corfu, F., J. M. Hanchar, P. W. O. Hoskin, and P. Kinny (2003), Atlas of zircon textures, *Rev. Mineral. Geochem.*, *53*, 468–500.

Crowley, J. L., J. S. Myers, P. J. Sylvester, and R. A. Cox (2005), Detrital zircon from the Jack Hills and Mount Narryer, Western Australia: Evidence for diverse >4.0 Ga source rocks, *J. Geol.*, *113*, 239–263.

Dawson, J. B., P. G. Hill, and P. D. Kinny (2001), Mineral chemistry of a zircon-bearing, composite, veined and metasomatised upper-mantle peridotite xenolith from kimberlite, *Contrib. Mineral. Petrol.*, *140*, 720–733.

Dunn, S. J., A. A. Nemchin, P. A. Cawood, and R. T. Pidgeon (2005), Provenance record of the Jack Hills metasedimentary belt: Source of the Earth's oldest zircons, *Precambrian Res.*, *138*, 235–254.

Ferry, J. M., and E. B. Watson (2007), New thermodynamic models and revised calibrations for the Ti-in-zircon and Zr-in-rutile thermometers, *Contrib. Mineral. Petrol*, in press.

Froude, D. O., T. R. Ireland, P. D. Kinny, I. S. Williams, W. Compston, and J. S. Myers (1983), Ion microprobe identification of 4,100–4,200 Myr-old terrestrial zircons, *Nature*, *304*, 616–618.

Fu, B., A. J. Cavosie, C. C. Clechenko, J. Fournelle, N. T. Kita, J. Lackey, F. Page, S. A. Wilde, and J. W. Valley (2005), Ti-in-zircon thermometer: Preliminary results, *Eos Trans. AGU*, *86*(52), Fall Meet. Suppl., Abstract V41F-1538.

Geisler, T., R. T. Pidgeon, R. Kurtz, W. van Bronswijk, and H. Schleicher (2003), Experimental hydrothermal alteration of partially metamict zircon, *Am. Mineral.*, *88*, 1496–1513.

Glikson, A. (2006), Comment on "Zircon thermometer reveals minimum melting conditions on earliest Earth" I, *Science*, *311*, 779a, doi:10.1126/science.1120073.

Harrison, T. M., J. Blichert-Toft, W. Müller, F. Albarede, P. Holden, and S. J. Mojzsis (2005a), Heterogeneous Hadean hafnium: Evidence of continental crust at 4.4 to 4.5 Ga, *Science*, *310*, 1947–1950.

Harrison, T. M., A. Aikman, P. Holden, A. M. Walker, C. McFarlane, D. Rubatto, and E. B. Watson (2005b), Testing the Ti-in-zircon thermometer, *Eos Trans. AGU*, *86*(52), Fall Meet. Suppl., Abstract V41F-1540.

Harrison, T. M., J. Blichert-Toft, W. Müller, F. Albarede, P. Holden, and S. J. Mojzsis (2006), Response to comment on "Heterogeneous Hadean hafnium: Evidence of continental crust at 4.4 to 4.5 Ga", *Science*, *312*, 1139b, doi:10.1126/science.1125408.

Harrison, T. M., E. B. Watson, and A. K. Aikman (2007), Temperature spectra of zircon crystallization in plutonic rocks, *Geology*, *35*, 635–638.

Hayden, L. A., E. B. Watson, and D. A. Wark (2005), Rutile saturation and TiO_2 diffusion in hydrous siliceous melts, *Eos Trans. AGU*, *86*(52), Fall Meet. Suppl., Abstract MR13A-0076.

Hoskin, P. W. O. (1998), Minor and trace element analysis of natural zircon ($ZrSiO_4$) by SIMS and laser ablation ICPMS: A consideration and comparison of two broadly competitive techniques, *J. Trace Microprobe Tech.*, *16*, 301–326.

Hoskin, P. W. O. (2005), Trace-element composition of hydrothermal zircon and the alteration of Hadean zircon from the Jack Hills, Australia, *Geochim. Cosmochim. Acta*, *69*, 637–648.

Hoskin, P. W. O., and L. P. Black (2000), Metamorphic zircon formation by solid-state recrystallization of protolith igneous zircon, *J. Metamorph. Geol.*, *18*, 423–439.

Hoskin, P. W. O., and T. R. Ireland (2000), Rare earth element chemistry of zircon and its use as a provenance indicator, *Geology*, *28*, 627–630.

Hoskin, P. W. O., P. D. Kinny, D. Wyborn, and B. W. Chappell (2000), Identifying accessory mineral saturation during differentiation in granitoid magmas: An integrated approach, *J. Petrol.*, *41*, 1365–1396.

Iizuka, T., K. Horie, T. Komiya, S. Maruyama, T. Hirata, H. Hidaka, and B. F. Windley (2006), 4.2 Ga zircon xenocryst in an Acasta gneiss from northwestern Canada: Evidence for early continental crust, *Geology*, *34*, 245–248.

Kamber, B. S., M. J. Whitehouse, R. Bolhar, and S. Moorbath (2005), Volcanic resurfacing and the early terrestrial crust: Zircon U-Pb and REE constraints from the Isua Greenstone Belt, southern West Greenland, *Earth Planet. Sci. Lett.*, *240*, 276–290.

Kemp, A. I. S., C. J. Hawkesworth, B. A. Paterson, and P. D. Kinny (2006), Episodic growth of the Gondwana supercontinent from hafnium and oxygen isotopes in zircon, *Nature*, *439*, 580–583.

Kerrich, R., and R. King (1993), Hydrothermal zircon and baddeleyite in Val d'Or Archean mesothermal gold deposits characteristics, compositions and fluid-inclusion properties, with implications for timing of primary gold mineralization, *Can. J. Earth Sci.*, *30*, 2334–2352.

King, E. M., C. T. Barrie, and J. W. Valley (1997), Hydrothermal alteration of oxygen isotope ratios in quartz phenocrysts, Kidd Creek Mine, Ontario: Magmatic values are preserved in zircon, *Geology*, *25*, 1079–1082.

Maas, R., P. D. Kinny, I. S. Williams, D. O. Froude, and W. Compston (1992), The Earth's oldest known crust: A geochronological and geochemical study of 3900–4200 Ma old detrital zircons from Mt. Narryer and Jack Hills, Western Australia, *Geochim. Cosmochim. Acta*, *56*, 1281–1300.

Manning, C. E., S. J. Mojzsis, and T. M. Harrison (2006), Geology, age and origin of supracrustal rocks, Akilia, Greenland, *Am. J. Sci.*, *306*, 303–366.

Markl, G. (2001), REE constraints on fractionation processes of massive-type anorthosites on the Lofoten Islands, Norway, *Mineral. Petrol.*, *72*, 325–351.

Miller, R. L., and J. S. Kahn (1962), *Statistical Analysis in the Geological Sciences*, 483 pp., John Wiley, New York.

Mojzsis, S. J., T. M. Harrison, and R. T. Pidgeon (2001), Oxygen-isotope evidence from ancient zircons for liquid water at the Earth's surface 4300 Myr ago, *Nature*, *409*, 178–181.

Moorbath, S., M. J. Whitehouse, and B. S. Kamber (1997), Extreme Nd-isotope heterogeneity in the early Archaean: Fact or fiction? Case histories from northern Canada and West Greenland, *Chem. Geol.*, *135*, 213–231.

Nelson, D. R., B. W. Robinson, and J. S. Myers (2000), Complex geological histories extending for ≥4.0 Ga deciphered from xenocryst zircon microstructures, *Earth Planet. Sci. Lett.*, *181*, 89–102.

Nemchin, A. A., R. T. Pidgeon, and M. J. Whitehouse (2006a), Re-evaluation of the origin and evolution of >4.2 Ga zircons from the Jack Hills metasedimentary rocks, *Earth Planet. Sci. Lett.*, *244*, 218–233.

Nemchin, A. A., M. J. Whitehouse, R. T. Pidgeon, and C. Myer (2006b), Oxygen isotopic signature of 4.4–3.9 Ga zircons as a monitor of differentiation processes on the Moon, *Geochim. Cosmochim. Acta.*, *70*, 1864–1872.

Nutman, A. P. (2006), Comment on "Zircon thermometer reveals minimum melting conditions on earliest Earth" II, *Science*, *311*, 779b, doi:10.1126/science.1120977.

Paces, J. B., and J. D. Miller (1993), Precise U-Pb ages of Duluth Complex and related mafic intrusions, northeastern Minnesota: Geochronological insights into physical, petrogenetic, and paleomagnetic and tectonomagnetic processes associated with the 1.1 Ga mid-continent rift system, *J. Geophys. Res.*, *98*, 13,997–14,013.

Peck, W. H., J. W. Valley, S. A. Wilde, and C. M. Graham (2001), Oxygen isotope ratios and rare earth elements in 3.3 to 4.4 Ga zircons: Ion microprobe evidence for high $\delta^{18}O$ continental crust and oceans in the early Archean, *Geochim. Cosmochim. Acta*, *65*, 4215–4229.

Peck, W. H., J. W. Valley, and C. M. Graham (2003), Slow oxygen diffusion rates in igneous zircons from metamorphic rocks, *Am. Mineral.*, *88*, 1003–1014.

Pettke, T., A. Audetat, U. Schaltegger, and C. A. Heinrich (2005), Magmatic-to-hydrothermal crystallization in the W-Sn mineralized Mole Granite (NSW, Australia). part II: Evolving zircon and thorite trace element chemistry, *Chem. Geol.*, *220*, 191–213.

Pidgeon, R. T., and S. A. Wilde (1998), The interpretation of complex zircon U-Pb systems in Archaean granitoids and gneisses from the Jack Hills, Narryer gneiss terrane, Western Australia, *Precambrian Res.*, *91*, 309–332.

Reymer, A. P. S., and G. Schubert (1985), Continental volume and freeboard through geological time, *Nature*, *316*, 336–339.

Rubatto, D. (2002), Zircon trace element geochemistry: Partitioning with garnet and the link between U-Pb ages and metamorphism, *Chem. Geol.*, *184*, 123–138.

Ryerson, F. J., and E. B. Watson (1987), Rutile saturation in magmas: Implications for Ti-Nb-Ta depletion in orogenic rock series, *Earth Planet. Sci. Lett.*, *86*, 225–239.

Samsonov, A. V., M. M. Bogina, E. V. Bibikova, A. Y. Petrova, and A. A. Shchipansky (2005), The relationship between adakitic, calc-alkaline volcanic rocks and TTGs: Implications for the tectonic setting of the Karelian greenstone belts, Baltic Shield, *Lithos*, *79*, 83–106.

Sano, Y., K. Terada, H. Hidaka, K. Yokoyama, and A. P. Nutman (1999), Palaeoproterozoic thermal events recorded in the ~4.0 Ga Acasta gneiss, Canada: Evidence from SHRIMP U-Pb dating of apatite and zircon, *Geochim. Cosmochim. Acta*, *63*, 899–905.

Schmitz, M. D., S. A. Bowring, and T. R. Ireland (2003), Evaluation of Duluth Complex anorthositic series (AS3) zircon as a U-Pb geochronological standard: New high-precision isotope dilution thermal ionization mass spectrometry results, *Geochim. Cosmochim. Acta*, *67*, 3665–3672.

Silverman, B. W. (1986), *Density Estimations for Statistics and Data Analysis*, *Monogr. Stat. Appl. Prob.*, vol. 26, 175 pp., Chapman and Hall, London.

Sun, S. S., and W. F. McDonough (1989), Chemical and isotopic systematics of oceanic basalts: Implications for mantle composition and processes, in *Magmatism in the Ocean Basins*, edited by A. D. Sanders and M. J. Norry, *Geol Soc. Spec. Publ.*, *42*, 313–345.

Taylor, H. P. (1968), The oxygen isotope geochemistry of igneous rocks, *Contrib. Mineral. Petrol.*, *19*, 1–71.

Taylor, H. P., and S. M. F. Sheppard (1986), Igneous rocks: I. Processes of isotopic fractionation and isotope systematics, *Rev. Mineral. Geochem.*, *16*, 227–271.

Tera, F., D. A. Papanastassiou, and G. J. Wasserburg (1974), Isotopic evidence for a terminal lunar cataclysm, *Earth Planet. Sci. Lett.*, *22*, 1–21.

Trail, D., S. J. Mojzsis, and T. M. Harrison (2004), Inclusion mineralogy of pre-4.0 Ga zircons from Jack Hills, Western Australia: A progress report (abstract), *Geochim. Cosmochim. Acta.*, *68*, A743.

Trail, D., S. J. Mojzsis, and T. M. Harrison (2007), Thermal events documented in Hadean zircons by ion microprobe depth profiles, *Geochim. Cosmochim. Acta*, in press.

Turner, G., T. M. Harrison, G. Holland, S. J. Mojzsis, and J. Gilmour (2004), Extinct Pu-244 in ancient zircons, *Science*, *306*, 89–91.

Valley, J. W. (2003), Oxygen isotopes in zircon, *Rev. Mineral. Geochem.*, *53*, 342–385.

Valley, J. W., J. R. Chiarenzelli, and J. M. McLelland (1994), Oxygen isotope geochemistry of zircon, *Earth Planet Sci. Lett.*, *126*, 187–206.

Valley, J. W., W. H. Peck, E. M. King, and S. A. Wilde (2002), A cool early Earth, *Geology*, *30*, 351–354.

Valley, J. W., I. N. Bindeman, and W. H. Peck (2003), Empirical calibration of oxygen isotope fractionation in zircon, *Geochim. Cosmochim. Acta*, *67*, 3257–3266.

Valley, J. W., et al. (2005), 4.4 billion years of crustal maturation: Oxygen isotope ratios of magmatic zircon, *Contrib. Mineral. Petrol.*, *150*, 561–580.

Valley, J. W., A. J. Cavosie, B. Fu, W. H. Peck, and S. A. Wilde (2006), Comment on "Heterogeneous Hadean hafnium: Evidence of continental crust at 4.4 to 4.5 Ga", *Science*, *312*, 1139a, doi:10.1126/science.1125301.

Vervoort, J. D., and J. Blichert-Toft (1999), Evolution of the depleted mantle: Hf isotope evidence from juvenile rocks through time, *Geochim. Cosmochim. Acta*, *63*, 533–556.

Watson, E. B., and D. J. Cherniak (1997), Oxygen diffusion in zircon, *Earth Planet. Sci. Lett.*, *148*, 527–544.

Watson, E. B., and T. M. Harrison (2005), New thermometer reveals minimum melting conditions on earliest Earth, *Science*, *308*, 841–844.

Watson, E. B., and T. M. Harrison (2006), Response to comments on "New thermometer reveals minimum melting conditions on earliest Earth", *Science*, *311*, 779c, doi:10.1126/science.1121080.

Watson, E. B., D. A. Wark, and J. B. Thomas (2006), Crystallization thermometers for zircon and rutile, *Contrib. Mineral. Petrol.*, *151*, 413–433.

Whitehouse, M. J., and B. S. Kamber (2002), On the overabundance of light rare earth elements in terrestrial zircons and its implication for Earth's earliest magmatic differentiation, *Earth Planet. Sci. Lett.*, *204*, 333–346.

Whitehouse, M. J., and B. S. Kamber (2003), A rare earth element study of complex zircons from early Archaean Amîtsoq gneisses, Godthåbsfjord, south-west Greenland, *Precambrian Res.*, *126*, 363–377.

Whitehouse, M. J., and B. S. Kamber (2005), Assigning dates to thin gneissic veins in high-grade metamorphic terranes: A cautionary tale from Akilia, southwest Greenland, *J. Petrol.*, *46*, 291–318.

Whitehouse, M. J., and J. P. Platt (2003), Dating high-grade metamorphism: Constraints from rare-earth elements in zircon and garnet, *Contrib. Mineral. Petrol.*, *145*, 61–74.

Wiedenbeck, M., et al. (2004), Further characterisation of the 91500 zircon crystal, *Geostand. Geoanal. Res.*, *28*, 9–39.

Wilde, S. A., J. W. Valley, W. H. Peck, and C. M. Graham (2001), Evidence form detrital zircons for the existence of continental crust and oceans 4.4 Ga ago, *Nature*, *409*, 175–178.

Young, E. D., M. L. Fogel, D. Rumble, and T. C. Hoering (1998), Isotope-ratio-monitoring of O_2 for microanalysis of $^{18}O/^{16}O$ and $^{17}O/^{16}O$ in geological materials, *Geochim. Cosmochim. Acta*, *62*, 3087–3094.

Zheng, Y. F., B. Fu, B. Gong, and L. Li (2003), Stable isotope geochemistry of ultrahigh pressure metamorphic rocks from the Dabie-Sulu orogen in China: Implications for geodynamics and fluid regime, *Earth Sci. Rev.*, *62*, 105–161.